

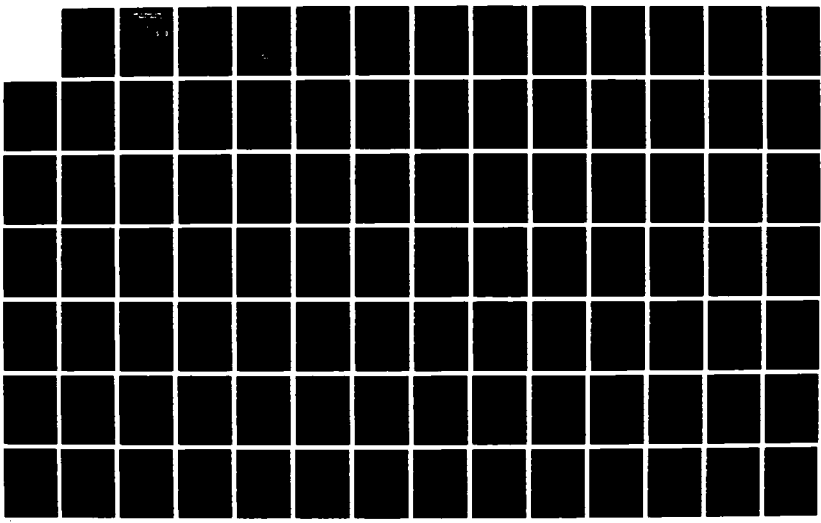
NO-RL90 189

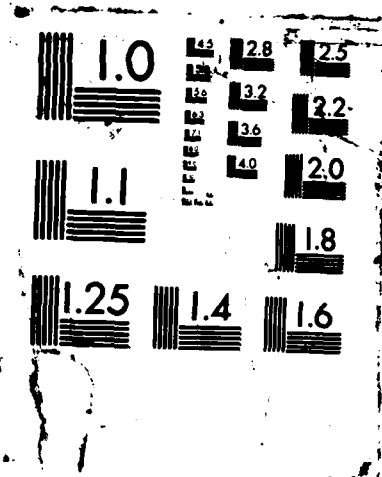
THEORETICAL MODEL OF THE CATHODE SPOT ON A UNIPOLAR ARC 1/2
(U) NAVAL POSTGRADUATE SCHOOL MONTEREY CA D H CURTISS
DEC 87

UNCLASSIFIED

F/G 20/3

ML





AD-A190 109

NAVAL POSTGRADUATE SCHOOL
Monterey, California

(2)
DTIC FILE COPY



THEESIS

DTIC
ELECTED
MAR 18 1988
S D
H

THEORETICAL MODEL OF THE CATHODE SPOT IN
A UNIPOLAR ARC

by

Dwayne H. Curtiss

December 1987

Thesis Advisor

F. Schwirzke

Approved for public release; distribution is unlimited.

88 3 16 026

REPORT DOCUMENTATION PAGE

1a. REPORT SECURITY CLASSIFICATION UNCLASSIFIED		1b. RESTRICTIVE MARKINGS			
2a. SECURITY CLASSIFICATION AUTHORITY		3. DISTRIBUTION/AVAILABILITY OF REPORT Approved for public release; distribution is unlimited.			
2b. DECLASSIFICATION/DOWNGRADING SCHEDULE					
4. PERFORMING ORGANIZATION REPORT NUMBER(S)		5. MONITORING ORGANIZATION REPORT NUMBER(S)			
6a. NAME OF PERFORMING ORGANIZATION Naval Postgraduate School	6b. OFFICE SYMBOL (if applicable) 33	7a. NAME OF MONITORING ORGANIZATION Naval Postgraduate School			
6c. ADDRESS (City, State, and ZIP Code) Monterey, California 93943-5000		7b. ADDRESS (City, State, and ZIP Code) Monterey, California 93943-5000			
8a. NAME OF FUNDING SPONSORING ORGANIZATION	8b. OFFICE SYMBOL (if applicable)	9. PROCUREMENT INSTRUMENT IDENTIFICATION NUMBER			
8c. ADDRESS (City, State, and ZIP Code)		10. SOURCE OF FUNDING NUMBERS			
		PROGRAM ELEMENT NO.	PROJECT NO.	TASK NO.	WORK UNIT ACCESSION NO.
11. TITLE (Include Security Classification) THEORETICAL MODEL OF THE CATHODE SPOT IN A UNIPOLAR ARC					
12. PERSONAL AUTHOR(S) Curtiss, Dwayne H.					
13a. TYPE OF REPORT Master's Thesis	13b. TIME COVERED FROM _____ TO _____	14. DATE OF REPORT (Year, Month, Day) 1987 December		15. PAGE COUNT 99	
16. SUPPLEMENTARY NOTATION					
17. COSATI CODES		18. SUBJECT TERMS (Continue on reverse if necessary and identify by block number) L (Thesis) Unipolar Arcing, Cathode Spot			
FIELD	GROUP	SUB-GROUP			
19. ABSTRACT (Continue on reverse if necessary and identify by block number) A theoretical study and computer analysis of the cathode spot of a unipolar arc was conducted. The underlying theories of Plasma Physics, Space Charge Effects, and Electron Emission needed for an understanding of cathode phenomena are presented. Two models of unipolar arcing are reviewed and an analysis of the cathode spot is begun. A stationary model of the cathode spot is formulated with a system of equations that is not closed. A method of solution, using the Steenbeck Minimum Principle, is utilized and a computer program developed to determine the cathode spot parameters. Results of the analysis are presented for arc currents of 100, 150, 175, 200, 300, and 400 Amperes. It is found that for copper stable arcs occur only for arc currents greater than 200 Amperes. <i>Comments: 100-400 A nice</i>					
20. DISTRIBUTION/AVAILABILITY OF ABSTRACT <input checked="" type="checkbox"/> UNCLASSIFIED/UNLIMITED <input type="checkbox"/> SAME AS RPT <input type="checkbox"/> DTIC USERS			21. ABSTRACT SECURITY CLASSIFICATION UNCLASSIFIED		
22a. NAME OF RESPONSIBLE INDIVIDUAL Prof. F. Schwirzke			22b. TELEPHONE (Include Area Code) 408-646-2635	22c. OFFICE SYMBOL Code 61Sw	

Approved for public release; distribution is unlimited.

Theoretical Model of the Cathode Spot in a Unipolar Arc

by

Dwayne H. Curtiss
Lieutenant, United States Navy
B.S., University of the State of New York, 1981

Submitted in partial fulfillment of the
requirements for the degree of

MASTER OF SCIENCE IN PHYSICS

from the

NAVAL POSTGRADUATE SCHOOL
December 1987

Author:

Dwayne H. Curtiss
Dwayne H. Curtiss

Approved by:

F. Schwirzke
F. Schwirzke, Thesis Advisor

K. E. Woehler.
K. E. Woehler, Second Reader

K. E. Woehler.
K. E. Woehler, Chairman,
Department of Physics

G. E. Schacher
G. E. Schacher,
Dean of Science and Engineering

ABSTRACT

A theoretical study and computer analysis of the cathode spot of a unipolar arc was conducted. The underlying theories of Plasma Physics, Space Charge Effects, and Electron Emission needed for an understanding of cathode phenomena are presented. Two models of unipolar arcing are reviewed and an analysis of the cathode spot is begun. A stationary model of the cathode spot is formulated with a system of equations that is not closed. A method of solution, using the Steenbeck Minimum Principle, is utilized and a computer program developed to determine the cathode spot parameters. Results of the analysis are presented for arc currents of 100, 150, 175, 200, 300, and 400 Amperes. It is found that for copper stable arcs occur only for arc currents greater than 200 Amperes.



Accession For	
NTIS GRA&I	<input checked="" type="checkbox"/>
DTIC TAB	<input type="checkbox"/>
Unannounced	<input type="checkbox"/>
Justification	
By _____	
Distribution/ _____	
Availability Codes	
Dist	Avail and/or Special
R-1	

TABLE OF CONTENTS

I.	INTRODUCTION.....	9
II.	BACKGROUND THEORY.....	11
	A. PLASMA PHYSICS.....	11
	1. Plasma Characteristics.....	11
	2. Debye Shielding.....	12
	3. Sheaths	14
	B. SPACE CHARGE LIMITED CURRENT FLOW.....	17
	1. Child-Langmuir Law.....	17
	2. Space Charge Limited Current in a Sheath.....	19
	3. MacKeown Equation.....	22
	C. ELECTRON EMISSION FROM METALS.....	24
	1. Thermionic-Field Emission.....	27
	2. Field-Thermionic Emission.....	29
	3. Intermediate Field-Thermionic Emission.....	31
	4. Explosive Electron Emission.....	32
III.	UNIPOLAR ARCING.....	34
	A. ROBSON-THONEMAN MODEL.....	34
	B. SCHWIRZKE-TAYLOR MODEL.....	37
IV.	CATHODE SPOTS.....	41
	A. TYPES OF CATHODE SPOTS.....	41
	B. THEORY OF STATIONARY CATHODE SPOTS.....	42
	1. Fundamental Equations	44

2. Method of Solution.....	48
V. COMPARISON OF THEORY AND EXPERIMENTAL DATA.....	51
VI CONCLUSIONS AND RECOMENDATIONS.....	73
LIST OF REFERENCES.....	74
APPENDIX A GENERAL EMISSION PROGRAM.....	77
APPENDIX B GENERAL EMISSION SUBROUTINE.....	79
APPENDIX C EMISSION APPLICABILITY SUBROUTINE.....	80
APPENDIX D T-F EMISSION SUBROUTINE.....	83
APPENDIX E FIELD-THERMIONIC EMISSION SUBROUTINE.....	85
APPENDIX F COMPLETE ELLIPTIC INTEGRAL OF THE 1ST KIND.....	87
APPENDIX G COMPLETE ELLIPTIC INTEGRAL OF THE 2ND KIND.....	89
APPENDIX H FOWLER-NORDHIEM ELLIPTIC FUNCTIONS.....	91
APPENDIX I INTERMEDIATE F-T EMISSION SUBROUTINE.....	92
APPENDIX J ARC PROGRAM.....	94
INITIAL DISTRIBUTION LIST.....	98

LIST OF TABLES

1 CATHODE SPOT MODEL CONSTANTS.....	51
2 CATHODE SPOT PARAMETERS FOR A 100 AMPERE ARC ON A COPPER CATHODE.....	54
3 CATHODE SPOT PARAMETERS FOR A 150 AMPERE ARC ON A COPPER CATHODE.....	57
4 CATHODE SPOT PARAMETERS FOR A 175 AMPERE ARC ON A COPPER CATHODE.....	60
5 CATHODE SPOT PARAMETERS FOR A 200 AMPERE ARC ON A COPPER CATHODE.....	63
6 CATHODE SPOT PARAMETERS FOR A 300 AMPERE ARC ON A COPPER CATHODE.....	66
7 CATHODE SPOT PARAMETERS FOR A 400 AMPERE ARC ON A COPPER CATHODE.....	69
8 CATHODE SPOT PARAMETERS FOR STABLE ARCS.....	72

LIST OF FIGURES

2.1	Plasma-Wall Interaction.....	15
2.2	Child-Langmuir Space Charge Limited Current Flow.....	20
2.3	MacKeown's Equation for Electric Field at the Cathode Surface.....	25
2.4	Potential Energy Diagram for a Metal-Vacuum Interface.....	26
2.5	Regions of Applicability for Thermionic, Field, and Intermediate Electron Emission Expressions	28
2.6	Electric Field Enhancement at a Whisker.....	33
3.1	Sheath Region Prior to Unipolar Arc Initiation.....	35
3.2	Sheath Region After Unipolar Arc Initiation.....	35
3.3	Schwirzke-Taylor Unipolar Arc Model.....	39
4.1	Model of the Cathode-Plasma Region.....	43
5.1	Cathode Spot Stability.....	52
5.2	Potentials for a 100 Ampere Arc.....	56
5.3	Potentials for a 150 Ampere Arc.....	59
5.4	Potentials for a 175 Ampere Arc.....	62
5.5	Potentials for a 200 Ampere Arc.....	65
5.6	Potentials for a 300 Ampere Arc.....	68
5.7	Potentials for a 400 Ampere Arc.....	71

ACKNOWLEDGMENTS

I would like to thank Professor Schwirzke for his guidance and constructive comments and Professor Woehler for showing me the world of Physics.

This would not have been possible without the loving support of my wife, Mary Alice and daughters, Katie and Erin. To them I am forever grateful for the joy they bring to my life.

I. INTRODUCTION

The study of cathode phenomena in gaseous discharges and electrical arcs has progressed over the last hundred years. In the last twenty years, this research has been revived as the interest in high power devices for pulsed power applications, switching devices, and nuclear fusion power generation has increased. The discovery in 1958 of a new form of electrical arc, one that burns between a metal plate and a dense plasma, called a unipolar arc has further increased interest in the cathode phenomena. For both the bipolar and unipolar arcs, the current transfer occurs in localized regions between a cathode and plasma which is referred to as the cathode spot. It has become increasingly apparent that the phenomena occurring in the cathode spot of a unipolar arc and that occurring in a bipolar arc are similar. Therefore, much of the theoretical work done on the cathode spot of a bipolar arc can be applied towards the understanding and formulation of a consistent theory of the unipolar arc.

This study will begin with a short review of some basic theories of plasma physics, space charge effects, and electron emission mechanisms. Two useful unipolar arcing models are then reviewed. The stationary cathode spot will then be studied and a set of equations presented that can be used to determine it's

parameters. It will be found that the system of equations is not closed, however, a method for the solution of the system can be formulated by using the Steenbeck Minimum Principle. Finally, results of calculations based on these equations is presented.

II. BACKGROUND THEORY

A. PLASMA PHYSICS

1. Plasma Characteristics

A plasma is formed when atoms are ionized into positive ions and negative electrons such that they form a gas. However, not all such gases are considered to be plasmas. A more complete definition of a plasma has been given by Chen [Ref. 1]:

"A plasma is a quasineutral gas of charged and neutral particles which exhibits collective behavior."

"Collective behavior" means that the behavior of a small region of the plasma is determined not only by conditions in the plasma that immediately surrounds it, but also by conditions in the plasma far away from it.

A plasma can be characterized by two quantities, n , the plasma density and T , the plasma temperature. Since the plasma must be quasineutral the density of ions, n_i , and the density of electrons, n_e , must be approximately equal. Therefore, the plasma density is defined as

$$n = n_e \approx n_i. \quad (\text{eqn. 2.1})$$

The plasma temperature is generally given in units of energy which corresponds to kT , where k is Boltzmann's constant and T is the plasma temperature in Kelvin. For a gas in thermal

equilibrium, which follows a Maxwellian distribution, the average energy of the gas particles is related to the plasma temperature by

$$E_{av} = \frac{3}{2} k T \quad (\text{eqn. 2.2})$$

where the plasma is assumed to be three dimensional

2. Debye Shielding

When a plasma is subjected to an external electric field the electrons and ions will drift in opposite directions. As they drift apart, they produce a charge separation and an internal electric field, which opposes the external field. The width of the region, over which the charge separation must occur to balance the external electric field, is proportional to the thermal energy of the plasma particles. If the dimension of the bulk plasma is greater than the dimension of the region over which this charge separation occurs, the interior of the plasma will be shielded from the external field.

The width of the charge separation can be determined, approximately, by considering a plasma where the ions are fixed in space, over the time frame of interest, and the electrons obey a Maxwellian distribution such that the Boltzman relation applies. Using Poisson's Equation in one dimension gives

$$\frac{d^2V}{dx^2} = -\frac{e}{\epsilon_0} (n_i - n_e) \quad (\text{eqn. 2.3})$$

where V is the electric potential and e is the electric charge. Since the ions are considered fixed, the density of ions will be constant and equal to the plasma density n_0 . The Boltzman relation then gives the electron distribution in the region of interest as

$$n_e = n_0 \exp\left(\frac{eV}{kT_e}\right). \quad (\text{eqn. 2.4})$$

Substituting equation 2.4 into equation 2.3 gives

$$\frac{d^2V}{dx^2} = \frac{en}{\epsilon_0} \left\{ \exp\left(\frac{eV}{kT_e}\right) - 1 \right\}. \quad (\text{eqn. 2.5})$$

To solve equation 2.5 the exponential can be expanded in a Taylor series, and neglecting terms of second order and higher gives

$$\frac{d^2V}{dx^2} = \frac{ne^2}{\epsilon_0 k T_e} V. \quad (\text{eqn. 2.6})$$

The solution of equation 2.6, which is a homogenous second order linear ordinary differential equation is given by

$$V = V_0 \exp\left(-\frac{|x|}{\lambda_D}\right) \quad (\text{eqn. 2.7})$$

where

$$\lambda_D = \sqrt{\frac{\epsilon_0 k T_e}{ne^2}}. \quad (\text{eqn. 2.8})$$

This quantity is known as the Debye Length and is a measure of the thickness of the shield that screens the bulk plasma from

the affect of external fields. This screening applies as long as the dimensions of the bulk plasma is much greater than the Debye Length.

3. Sheaths

When a plasma comes in contact with a wall, the electrons and ions that hit the wall will recombine. But since the electrons are moving at a higher velocity than the ions, the electrons will be lost faster than the ions resulting in a net positive charge at the plasma-wall boundary. The wall will then be at a lower potential than the bulk plasma and an electric field will exist. Figure 2.1 illustrates the potential variation in a plasma which is in contact with a wall. Due to Debye Shielding a layer of charge separation will exist, called the sheath, which will isolate the bulk plasma from this potential difference. The effect of the sheath is to accelerate the ions and to decelerate the electrons that enter the region until the flux of ions is balanced by the flux of electrons. Therefore, only those electrons in the high energy tail of the velocity distribution will be energetic enough to cross the sheath and all others will be repelled back into the plasma.

The variation of the potential in the plasma sheath will now be considered. In order to simplify the problem the following assumptions will be made:

- * The ions enter the sheath region with a drift velocity u_0 .
- * The ions have $T_i=0$ so that all ions have a velocity u_0 at the plasma-sheath boundary,

- * The sheath region is collisionless and in steady state,
- * The potential decreases monotonically with x ,
- * The electrons follow the Boltzman relation (equation 2.4).

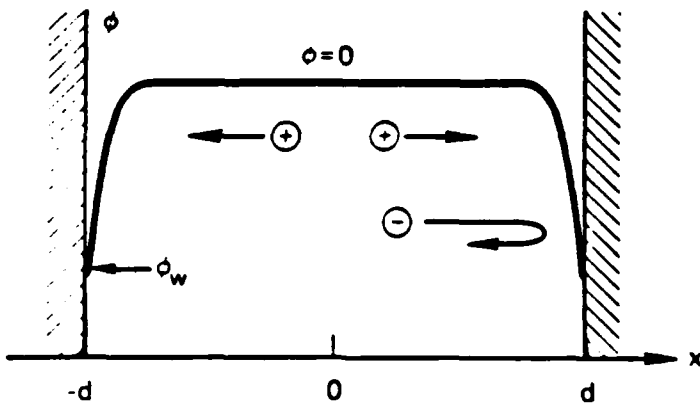


Figure 2.1 Plasma-Wall Interaction

Applying conservation of energy to the ions in the sheath region gives

$$\frac{1}{2}Mu^2 = \frac{1}{2}Mu_0^2 - eV(x). \quad (\text{eqn. 2.9})$$

Solving equation 2.9 for the ion velocity gives

$$u = \sqrt{u_0^2 - \frac{2eV}{M}}. \quad (\text{eqn. 2.10})$$

The ion density within the sheath is determined from the ion equation of continuity which is given by

$$n_i(x)u(x) = n_0u_0. \quad (\text{eqn. 2.11})$$

Using equation 2.10 for the ion velocity, equation 2.11 can be solved for the ion density which gives

$$n_i(x) = n_0 \left(1 - \frac{2eV}{u_0^2 M} \right)^{-\frac{1}{2}} \quad (\text{eqn. 2.12})$$

Substituting equation 2.4 and 2.12 into equation 2.3 gives

$$\frac{d^2V}{dx^2} = \frac{en_0}{\epsilon_0} \left[\exp\left(\frac{eV}{kT_s}\right) - \left(1 - \frac{2eV}{u_0^2 M} \right)^{-\frac{1}{2}} \right]. \quad (\text{eqn. 2.13})$$

Equation 2.13 is the non-linear planar sheath equation. By multiplying each side by the first derivative of the potential the equation can be integrated once to give

$$V'^2 - V_0'^2 = \frac{2n_0 k T_s}{\epsilon_0} \left\{ \left[\exp\left(\frac{eV}{kT_s}\right) - 1 \right] + \frac{Mu_0^2}{kT_s} \left[\left(1 - \frac{2eV}{Mu_0^2} \right)^{\frac{1}{2}} - 1 \right] \right\}. \quad (\text{eqn. 2.14})$$

Further solution of equation 2.14 would require numerical methods. If the electric field inside the plasma is zero, then the first derivative of the potential inside the plasma must also be zero. The left hand side of equation 2.14 is therefore greater than zero, and the following inequality results

$$\exp\left(\frac{eV}{kT_s}\right) - 1 + \frac{Mu_0^2}{kT_s} \left[\left(1 - \frac{2eV}{Mu_0^2} \right)^{\frac{1}{2}} - 1 \right] > 0. \quad (\text{eqn. 2.15})$$

This inequality can be greatly simplified by expanding the left hand terms in Taylor series expansions and neglecting terms of third order and higher. The resulting inequality is known as the Bohm sheath criterion and is given by

$$u_0 > \sqrt{\frac{kT_e}{M}}. \quad (\text{eqn. 2.16})$$

This requires that the ions must enter the sheath region with a velocity greater than the ion acoustic velocity of the plasma. In order for this to occur, there must be a finite electric field within the plasma. Therefore, the assumption that the potential and the electric field are zero at the plasma-sheath boundary is only an approximation.

B. SPACE CHARGE LIMITED CURRENT FLOW

1. Child-Langmuir Law

The current that can flow between the cathode and anode of a vacuum diode is limited by the space charge of the electrons that exist between them. The electrons distort the external field and thereby reduce and can even reverse the field at the cathode surface.

As an example, consider a diode consisting of infinite flat plates separated by a distance d . Assume that there is an unlimited supply of electrons available from the cathode, and that the initial velocity of the electrons after emission is negligible compared with the velocity that they will gain while

crossing the electrode gap. The kinetic energy of the electrons crossing the gap and the current density carried by the electrons is given by

$$\frac{1}{2}mv^2 = eV \quad (\text{eqn. 2.17})$$

and

$$j = env. \quad (\text{eqn. 2.18})$$

Using Poisson's equation, in one dimension, the current-voltage relationship can be derived as follows:

$$\frac{d^2V(x)}{dx^2} = \frac{en(x)}{\epsilon_0}. \quad (\text{eqn. 2.19})$$

The electron velocity is determined from equation 2.17 to be

$$v(x) = \sqrt{\frac{2e}{m}}V^{\frac{1}{2}}. \quad (\text{eqn. 2.20})$$

The electron density is determined using equation 2.18 and 2.20, and after substituting into equation 2.19 gives

$$\frac{d^2V}{dx^2} = \frac{j}{\epsilon_0}\sqrt{\frac{m}{2e}}V^{-\frac{1}{2}}. \quad (\text{eqn. 2.21})$$

In order to solve equation 2.21 both sides are multiplied by the first derivative of the potential and reduced to the following form

$$\frac{d}{dx}\left(\frac{dV}{dx}\right)^2 = \frac{j}{\epsilon_0}\sqrt{\frac{2m}{e}}V^{-\frac{1}{2}}\frac{dV}{dx}. \quad (\text{eqn. 2.22})$$

Equation 2.22 is then integrated over the gap using the boundary conditions that the electric field and the potential are zero at the cathode. The result of this integration gives

$$\frac{dV}{dx} = \sqrt{\frac{2j}{\epsilon_0}} \sqrt{\frac{2m}{e}} V. \quad (\text{eqn. 2.23})$$

Integrating once again over the gap, applying the boundary conditions, and rearranging gives the desired current-voltage relationship of

$$j = \frac{4\sqrt{2}\epsilon_0}{9} \sqrt{\frac{e}{m}} V^{\frac{3}{2}}. \quad (\text{eqn. 2.24})$$

Equation 2.24 is known as the Child-Langmuir Law for space charge limited current flow [Ref. 2]. Although it has been derived here using simple assumptions, the proportionality of the current density to the 3/2 power of the potential difference remains for more difficult geometries under non-relativistic conditions. It should also be pointed out that the Child-Langmuir Law applies to both positive and negative charge carriers. Figure 2.2 is a plot of electron current density versus potential for several gap widths.

2. Space Charge Limited Current in a Sheath

In deriving the planar sheath equation it was assumed that the electron density followed the Boltzman relation equation 2.4. Therefore, in a region close to the wall the electron density will be much less than the ion density

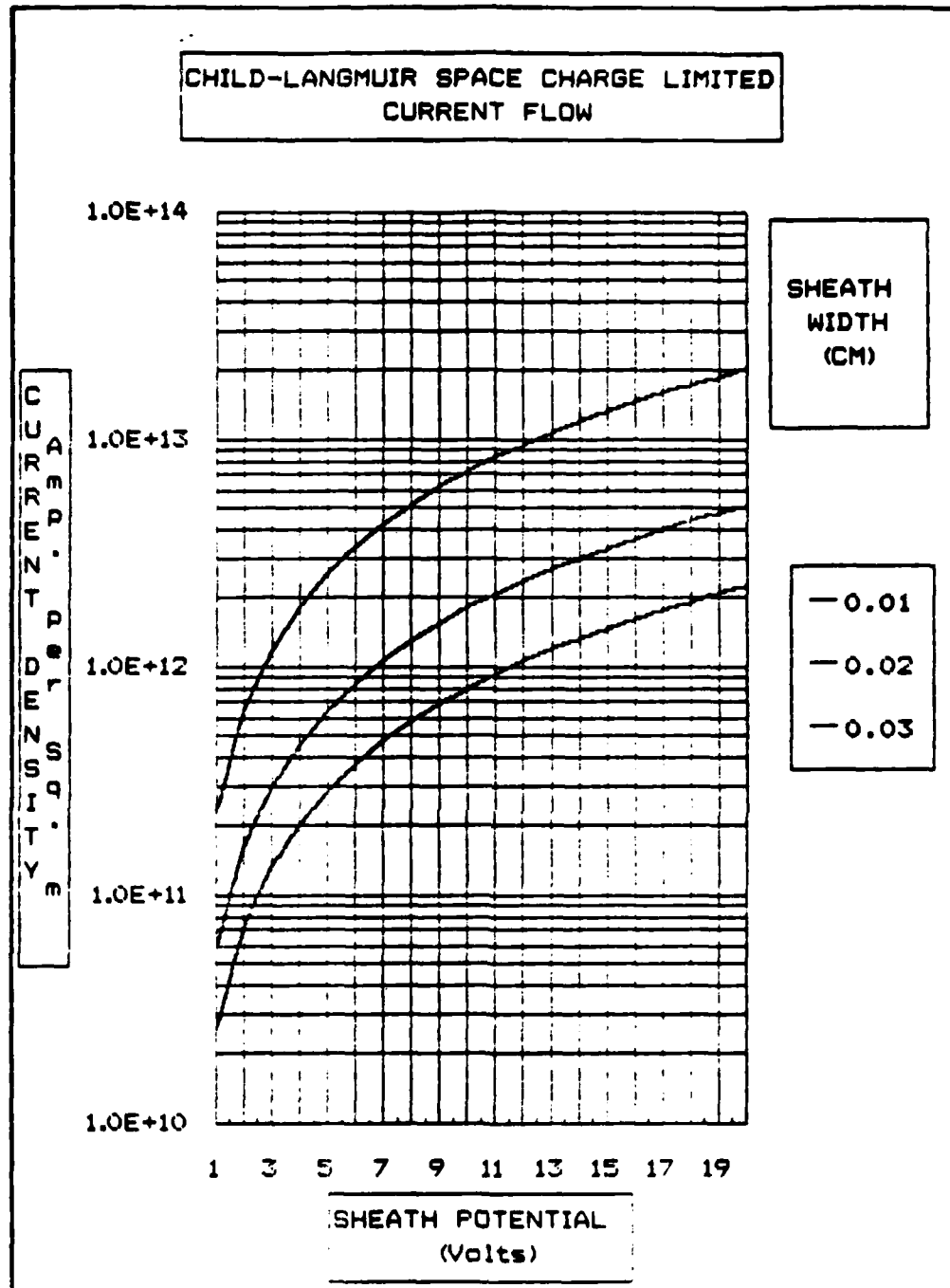


Figure 2.2 Child-Langmuir Space Charge Limited Current Flow

and can be neglected. The first derivative of the potential at the point in the sheath where the electron density can be neglected, is also assumed to be negligible compared with the slope of the potential near the wall. Equation 2.13 then reduces to

$$\frac{d^2V}{dx^2} = -\frac{en_0}{\epsilon_0} \left(1 - \frac{2eV}{u_0^2 M}\right)^{-\frac{1}{2}}. \quad (\text{eqn. 2.25})$$

Making the change of variable that $V = -v$ and noting that

$$\frac{2eV}{u_0^2 M} \gg 1 \quad (\text{eqn. 2.26})$$

equation 2.25 reduces to

$$\frac{d^2V}{dx^2} \approx \frac{en_0 u_0}{\epsilon_0} \sqrt{\frac{M}{2e}} V^{-\frac{1}{2}}. \quad (\text{eqn. 2.27})$$

The ion current density is constant across the sheath and is given by

$$j_i = en_0 u_0. \quad (\text{eqn. 2.28})$$

After substituting equation 2.28 into equation 2.27, the resulting expression is the same as equation 2.21. Therefore, the solution of equation 2.27 for the ion current density results in the Child-Langmuir Law for space charge limited current flow, equation 2.24.

3. MacKeown Equation

In an arc, the current is carried primarily by the electrons emitted by the cathode and by a smaller amount of positive ions flowing from the plasma to the cathode. If the space charge, which causes the cathode drop in the plasma sheath, is high enough it may exert a strong electric field at the surface of the cathode. This can then result in a large field emission current in addition to any thermionic current.

The electric field at the cathode surface can be determined using Poisson's Equation. The following derivation measures distance and potential difference from inside the plasma where the cathode drop begins. The electron and ion current densities are given by

$$j_e = e n_e v \quad (\text{eqn. 2.29})$$

and

$$j_i = e n_i u. \quad (\text{eqn. 2.30})$$

Substituting equation 2.29 and 2.30 into equation 2.3 gives

$$\frac{d^2V}{dx^2} = -\frac{1}{\epsilon_0} \left(\frac{j_i}{u} - \frac{j_e}{v} \right) \quad (\text{eqn. 2.31})$$

where V is the potential difference, j_i , the ion current density, j_e , the electron current density, u, the ion velocity, and v, the electron velocity.

The velocity of the ions and electrons are determined using the conservation of energy. The initial energies are

neglected, based on the assumption that the energy gained by the ions and electrons in crossing the sheath are much greater than the initial energies. For the ions the energy balance is

$$\frac{1}{2}Mu^2 = eV \quad (\text{eqn. 2.32})$$

and for the electrons the energy balance gives

$$\frac{1}{2}mv^2 = e(V_c - V) \quad (\text{eqn. 2.33})$$

where M is the mass of the positive ion, m, the mass of the electron and V_c is the potential of the cathode. Substituting equation 2.32 and 2.33 into equation 2.31 gives

$$\frac{d^2V}{dx^2} = -\frac{1}{\epsilon_0} \left[j_i \left(\frac{M}{2eV} \right)^{\frac{1}{2}} - j_e \left(\frac{m}{2e(V_c - V)} \right)^{\frac{1}{2}} \right]. \quad (\text{eqn. 2.34})$$

Multiplying both sides by the first derivative of the potential difference, equation 2.30 can be integrated once and gives

$$F^2 = \frac{4}{\epsilon_0} \left\{ j_i \left(\frac{MV}{2e} \right)^{\frac{1}{2}} + j_e \left(\frac{m(V_c - V)}{2e} \right)^{\frac{1}{2}} - j_e \left(\frac{mV_c}{2e} \right)^{\frac{1}{2}} \right\} \quad (\text{eqn. 2.35})$$

where F is the electric field. Evaluating for V = V_c gives the electric field at the cathode surface as

$$F^2 = \frac{4}{\epsilon_0} \left(\frac{MV_c}{2e} \right)^{\frac{1}{2}} j_i \left\{ 1 - \frac{j_e}{j_i} \left(\frac{m}{M} \right)^{\frac{1}{2}} \right\}. \quad (\text{eqn. 2.36})$$

Equation 2.36 is known as Mackeown's Equation [Ref. 3] and can be used to determine the electric field existing at the cathode provided the values of the cathode drop, the ion current density, and the electron current density are known. Figure 2.3 is a plot of electric field at the cathode surface versus ion current density for several ratios of electron to ion current densities.

C. ELECTRON EMISSION FROM METALS

The theory of electron emission from metals is very well understood. The basic processes have been explained on the basis of a free electron gas in the metal, that is described by Fermi-Dirac statistics, and a potential barrier at the metal surface. Figure 2.4 shows a typical potential energy diagram for an electron as a function of distance from the metal-vacuum interface. For thermionic emission, that is emission at high temperature and low electric field, the electrons are emitted predominately by passing over the potential barrier at the metal surface. For field emission, that is emission at low temperature and high electric field, the electrons are emitted predominately by tunneling through the potential barrier.

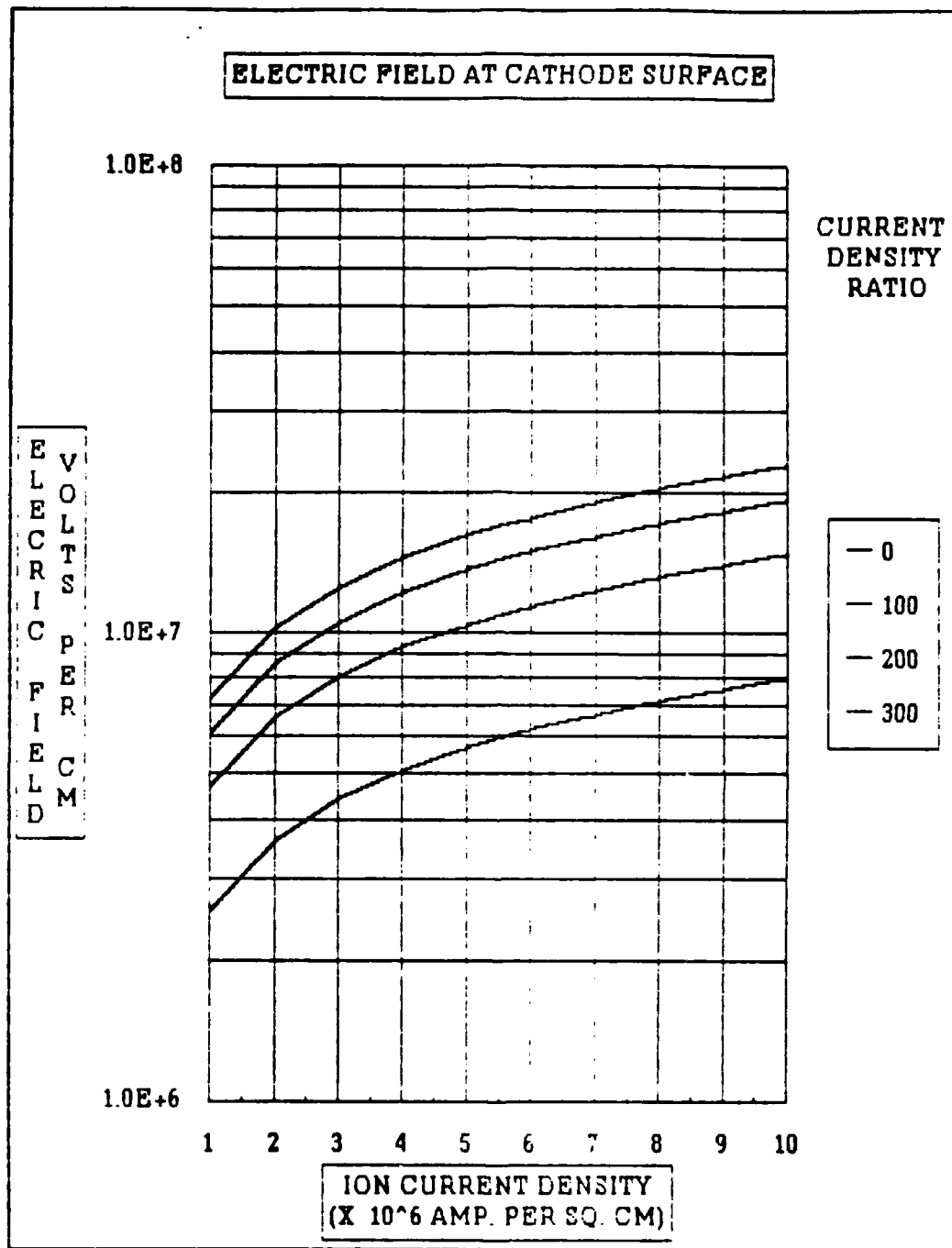


Figure 2.3 MacKeown's Equation for Electric Field at the Cathode Surface

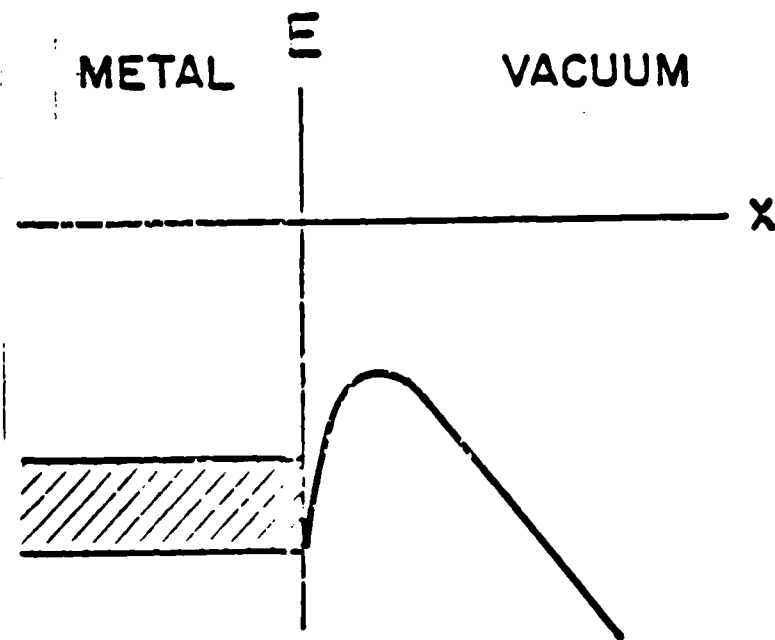


Figure 2.4 Potential Energy Diagram for a Metal-Vacuum Interface

In the past, thermionic and field emission have been treated separately, which has resulted in the well known Richardson equation for thermionic emission, and the Fowler-Nordheim equation for field emission. The expressions that will be used here, however, are based on an approach that treats both thermionic and field emission from a unified point of view [Ref. 4].

Hartree units are used in the following sections because they greatly simplify the expressions. Thus the following quantities are redefined as:

$$j^* = j \frac{m^3 e^*}{(4\pi\epsilon_0)^* \hbar^*}, \quad (\text{eqn. 2.37})$$

$$F^* = F \frac{m^2 e^3}{(4\pi\epsilon_0)^3 \hbar^4}, \quad (\text{eqn. 2.38})$$

$$(kT)^* = (kT) \frac{me^4}{(4\pi\epsilon_0)^2 \hbar^2}, \quad (\text{eqn. 2.39})$$

$$\phi^* = \phi \frac{me^4}{(4\pi\epsilon_0)^2 \hbar^2}, \quad (\text{eqn. 2.40})$$

where the starred quantities on the left are in SI units and their respective counterparts on the right are in Hartree units.

The following sections will give expressions that can be used to determine the current density that can be expected to be emitted from a metal given the surface temperature, the electric field at the surface, and the work function for the metal under consideration. In addition, a set of applicability conditions are given that can be used to determine the validity of the particular expression for a given situation. Figure 2.5 illustrates the regions of applicability of the emission equations on a plot of temperature versus electric field. Appendix A is a Fortran program that calculates the current density that can be expected to be emitted. Appendix B and C are Fortran subroutines that calculate the current density and applicability of the expressions to be used respectively.

1 Thermionic-Field Emission

The current density that can be expected from thermionic emission, corrected for the Schottky effect, is given by

$$j = \frac{1}{2\pi^2} (kT)^2 \left(\frac{\pi d}{\sin \pi d} \right) \exp \left[-\frac{\left(\phi - F^{\frac{1}{2}} \right)}{kT} \right] \quad (\text{eqn. 2.41})$$

where

$$d = \frac{F^{\frac{3}{4}}}{\pi kT}. \quad (\text{eqn. 2.42})$$

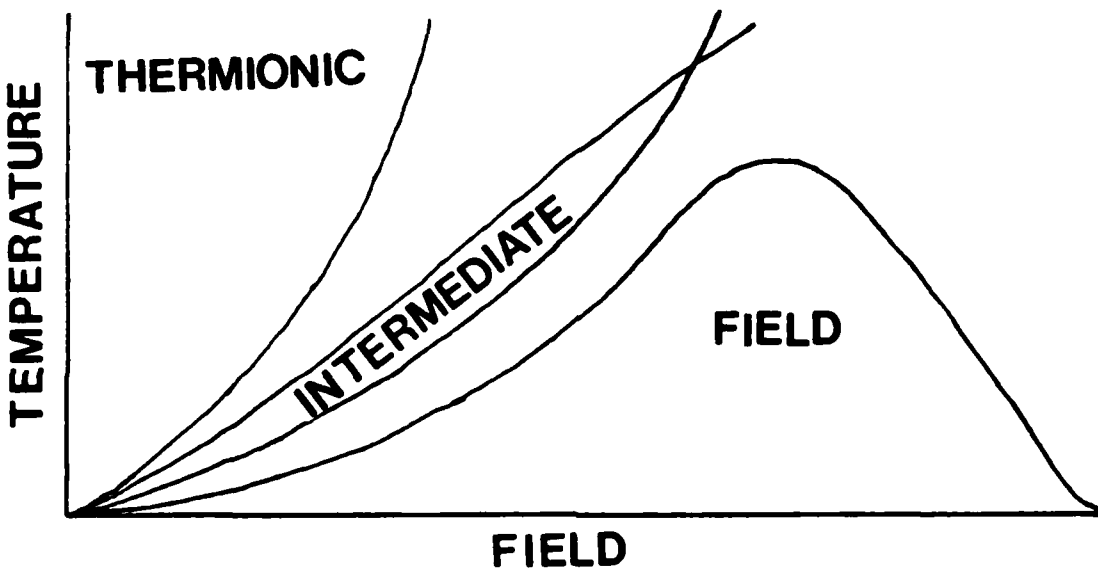


Figure 2.5 Regions of Applicability for Thermionic, Field, and Intermediate Electron Emission Expressions

For equation 2.41 to be applicable the following conditions must be satisfied:

$$\ln \left\{ \frac{(1-d)}{d} \right\} - \frac{1}{d(1-d)} > -\pi F^{-\frac{3}{4}} \left(\phi - F^{\frac{1}{2}} \right), \quad (\text{eqn. 2.43})$$

$$\ln\left(\frac{(1-d)}{d}\right) - \frac{1}{(1-d)} > -\pi F^{-\frac{1}{6}}. \quad (\text{eqn. 2.44})$$

Equation 2.41 reduces to the Richardson equation in the limit as the electric field is reduced toward zero. Appendix D is a listing of a Fortran subroutine that calculates the Thermionic-Field emission current density based on equation 2.41.

2. Field-Thermionic Emission

The current density that can be expected from field emission, corrected for temperature, is given by

$$J = \frac{F^2}{16\pi^2\phi t^2} \left(\frac{\pi ckT}{\sin \pi ckT} \right) \exp\left(-\frac{4\sqrt{2}\phi^{\frac{3}{2}}v}{3F}\right) \quad (\text{eqn. 2.45})$$

where

$$t(y) = \frac{1}{1+y} \left\{ (1+y)E\left[\sqrt{\frac{1-y}{1+y}}\right] - yK\left[\sqrt{\frac{1-y}{1+y}}\right] \right\}, \quad (\text{eqn. 2.46})$$

$$c = 2\sqrt{2}\frac{\phi^{\frac{1}{2}}}{F}t(y), \quad (\text{eqn. 2.47})$$

$$v(y) = -\sqrt{\frac{y}{2}} \left\{ -2E\left[\sqrt{\frac{y-1}{2y}}\right] + (y+1)K\left[\sqrt{\frac{y-1}{2y}}\right] \right\}$$

for $y > 1$, (eqn. 2.48)

$$v(y) = \sqrt{1+y} \left\{ E\left[\sqrt{\frac{1-y}{1+y}}\right] - yK\left[\sqrt{\frac{1-y}{1+y}}\right] \right\}$$

for $y < 1$, (eqn. 2.49)

$$y = \frac{F^{\frac{1}{2}}}{\phi}. \quad (\text{eqn. 2.50})$$

Equations 2.46, 2.48, and 2.49 are the Fowler-Nordheim Elliptic functions. The functions $K[k]$ and $E[k]$ are complete elliptic integrals of the first and second kind respectively and are defined as

$$K[k] = \int_0^{\frac{\pi}{2}} (1 - k^2 \sin^2 \theta)^{-\frac{1}{2}} d\theta, \quad (\text{eqn. 2.51})$$

$$E[k] = \int_0^{\frac{\pi}{2}} (1 - k^2 \sin^2 \theta)^{\frac{1}{2}} d\theta. \quad (\text{eqn. 2.52})$$

For equation 2.45 to be applicable the following conditions must be satisfied:

$$\phi - F^{\frac{1}{2}} > \frac{F^{3/4}}{\pi} + \frac{kT}{1 - ckT}, \quad (\text{eqn. 2.53})$$

$$1 - ckT > \sqrt{2f}kT, \quad (\text{eqn. 2.54})$$

$$f = \frac{\sqrt{2}\phi^{\frac{1}{2}}}{2F(\phi^2 - F)} v(y). \quad (\text{eqn. 2.55})$$

Equation 2.45 reduces to the Fowler-Nordheim equation in the limit as the temperature approaches zero. Appendix E is a listing of a Fortran subroutine that calculates the Field-Thermionic current density based on equation 2.45. This subroutine makes calls to the subroutines listed in Appendix F, G, and H, which are used to calculate the Complete Elliptic Integral of the First Kind, Complete Elliptic Integral of the Second Kind, and the Fowler-Nordheim Elliptic functions respectively.

3. Intermediate Field-Thermionic Emission

When equations 2.41 and 2.45 are not applicable, the current density from field-thermionic emission may be determined in the intermediate region as

$$j = \frac{F}{2\pi} \left(\frac{kTt}{2\pi} \right)^{\frac{1}{2}} \exp \left(-\frac{\phi}{kT} + \frac{F^2 \theta}{24(kT)^3} \right) \quad (\text{eqn. 2.56})$$

where

$$\theta = \frac{3}{t^2} - \frac{2v}{t^3}. \quad (\text{eqn. 2.57})$$

The argument of the functions t , equation 2.46, and v , equations 2.48 and 2.49, as used in equations 2.56 and 2.57, is given by

$$y_* = \frac{F^{\frac{1}{2}}}{(-\eta)}. \quad (\text{eqn. 2.58})$$

η can be determined by solving the following equation by iteration:

$$\eta = -\frac{F^2}{8(kT)^2 t^2(y_*)}. \quad (\text{eqn. 2.59})$$

For equation 2.56 to be applicable the following conditions must be satisfied:

$$\frac{1}{y_*} > 1 + \frac{F^{1/4} d}{\pi(d-1)}, \quad (\text{eqn. 2.60})$$

$$d = \frac{2\sqrt{2}t(y_*)}{\pi\sqrt{y_*}}, \quad (\text{eqn. 2.61})$$

$$-\frac{F^2}{8(kT)^2 t_n^2} > -\phi + \frac{kT}{1 - F \left(2\sqrt{2}\phi^{\frac{1}{2}} kT t_n \right)^{-1}}. \quad (\text{eqn. 2.62})$$

Appendix I is a listing of a Fortran subroutine that calculates the intermediate Field-Thermionic emission current density based on equation 2.56.

4. Explosive Electron Emission

The emission mechanisms discussed so far have wide applicability to many physical devices. However, with the advent of high current cathodes the thermionic and field emission theories were unable to explain the high current densities observed. One explanation for this high current density is that the surface of the cathode is not smooth, but actually has a surface covered with micropoints, or whiskers. The significance of the whisker is that the electric field, at the surface of the whisker is enhanced by a factor of 10 - 1000. Figure 2.6 illustrates the electric field enhancement that can occur at the tip of a whisker. This results in a higher field emission current density from the whisker, and ultimately leads to explosive destruction of the emission site. This destruction produces a local burst of plasma that expands rapidly away from the cathode surface and has therefore come to be known as a cathode flare or plasma jet. The electrons, that reach the anode, are then emitted from the surface of the plasma jet. This whole process is commonly referred to as explosive electron emission [Refs. 5 and 6].

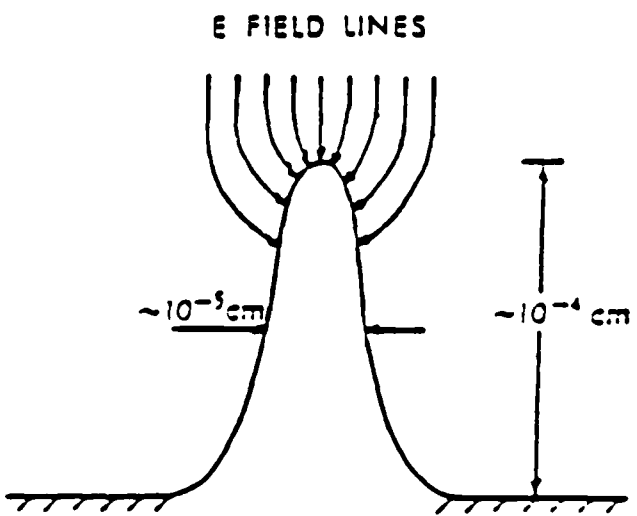


Figure 2.6 Electric Field Enhancement at a Whisker

Fursei and Zhukov [Refs. 7, 8, and 9] have experimentally characterized the explosive emission process and have confirmed the existence of micropoints and that the current density follows the Fowler-Nordheim field emission theory with the inclusion of a field enhancement factor.

III. UNIPOLAR ARCING

A. Robson-Thonemann Model

In 1958, Robson and Thoneman observed an electrical arc burning between a dense hot plasma and a metal wall [Ref. 10]. What made this unusual was that there was no anode present to collect the electrons emitted from the conducting wall. Apparently, the wall was acting as both a cathode and anode, and therefore, they named what they observed a "unipolar arc."

Robson and Thoneman proposed the following model to explain the occurrence of unipolar arcing. When a hot dense plasma comes in contact with a conducting wall a sheath will form. If the plasma temperature is high, the sheath or floating potential can exceed that necessary to initiate an electric arc. A cathode spot, which is a local center of emission, could then form on the metal surface. The large electron current flow into the plasma from the arc would result in lowering the plasma potential to the cathode fall potential of the arc. This allows more electrons from the high energy tail of the velocity distribution to cross the sheath and recombine at the wall and thus closing the current loop. Figure 3.1 illustrates the situation in the sheath prior to initiation of an arc, and Figure 3.2 shows the return current flow after arc initiation.

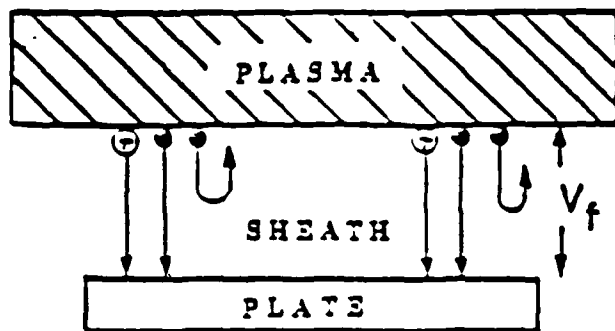


Figure 3.1 Sheath Region Prior to Unipolar Arc Initiation

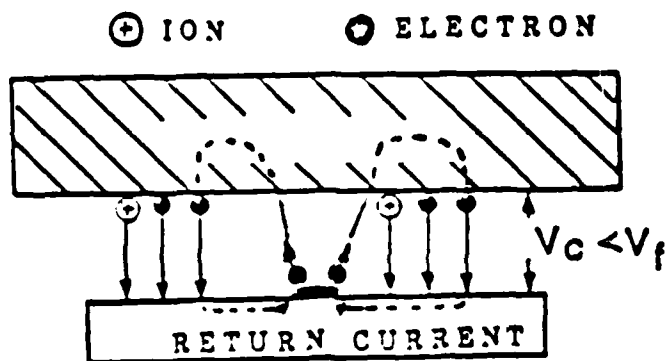


Figure 3.2 Sheath Region After Unipolar Arc Initiation

The resulting change in current flow outside of the arc is then given by

$$I = Aen \left(\frac{kT_e}{2\pi m} \right)^{\frac{1}{2}} \left\{ \exp\left(-\frac{eV_c}{kT_e}\right) - \exp\left(-\frac{eV_f}{kT_e}\right) \right\} \quad (\text{eqn. 3.1})$$

where I is the current, A is the area of the metal plate, and V_c is the cathode drop of the arc. But since the net current flow between the plasma and the wall must be zero, equation 3.1 also gives the current flow inside the arc.

The ion current density in the sheath can be approximated as

$$j_i \approx en_0 \sqrt{\frac{kT_e}{M}} \quad (\text{eqn. 3.2})$$

where the Bohm sheath criterion is used to approximate the ion velocity. The electron current density in the sheath can be determined by noting that the net flux of electrons, *, from the plasma into the sheath is given by

$$\Phi = \frac{1}{4} n_e \bar{v}. \quad (\text{eqn. 3.3})$$

Using the Boltzman relation for the electron density and the expression for the average speed of particles following a Maxwellian distribution gives

$$j_e = \frac{1}{4} en_0 \exp\left(\frac{eV_s}{kT_e}\right) \sqrt{\frac{8kT_e}{\pi m}}. \quad (\text{eqn. 3.4})$$

The net current density across the sheath must be zero. Therefore, setting equation 3.2 equal to equation 3.4, and solving for the sheath potential gives

$$V_s = \frac{kT_e}{2e} \ln\left(\frac{M}{2\pi m}\right). \quad (\text{eqn. 3.5})$$

Robson and Thoneman point out that there is a minimum current necessary to maintain an arc burning. Therefore, according to equation 3.1, if the plate area is small enough a unipolar arc can not occur. For example, using copper with a plasma temperature of 4 eV, a cathode fall potential of 15 V, a plasma density of 10^{13} cm^{-3} , and an arc current of 100 amperes would require a plate area of 115 cm^2 . For a circular area, the radius required is 6.05 cm.

B. Schwirzke-Taylor Model

Schwirzke and Taylor have expanded on the basic concepts of the Robson-Thoneman model [Ref. 11]. They propose that for an arc to occur, the ion density above the cathode spot must increase to allow for the arc current to flow. This is contrary to the Robson-Thoneman model which assumes a constant plasma density. Once a cathode spot forms the desorption of neutral atoms and evaporation of the metal atoms from the spot is greatly increased. If only a small fraction of these neutral atoms become ionized in the sheath the plasma density will increase above the cathode spot. Thus, according to equation 2.8 the Debye length will decrease resulting in a decrease of the sheath width above the cathode spot. The electric field above the spot increases, where the field can be approximated as

$$|F_n| \approx \frac{V_f}{\lambda_D} = \sqrt{\pi n_e k T_e} \ln \left(\frac{M}{2\pi m} \right). \quad (\text{eqn. 3.6})$$

Schwirzke [Refs. 12 and 13] elaborates further on the electric fields set up inside the high density plasma which forms above the spot. The fluid equation of motion of the electrons in the plasma is given by

$$n_e m \frac{d\vec{v}_e}{dt} = -en_e (\vec{F} + \vec{v}_e \times \vec{B}) - \nabla P_e + \frac{en_e}{\sigma} \vec{j}. \quad (\text{eqn. 3.7})$$

The time derivative can be neglected over the time span of an arc, and further assuming no magnetic field, equation 3.7 can be solved for the electric field, which gives

$$\vec{F} = \frac{\vec{j}}{\sigma} - \frac{1}{en_e} \nabla P_e. \quad (\text{eqn. 3.8})$$

The first term on the right hand side of equation 3.8 can be neglected in a weakly ionized plasma. This implies that the mean free path length for collision between the electrons and the neutral atoms is much greater than the dimensions of the region of increased density above the cathode spot. Thus, the increased plasma pressure above the spot creates a radial electric field given by

$$\vec{F}_r = -\frac{1}{en_e} \nabla P_e = -\frac{kT_e}{en_e} \nabla n_e. \quad (\text{eqn. 3.9})$$

The affect of this radial electric field is to lower the plasma potential in a ring around the cathode spot. The change in the potential can be determined by integrating equation 3.9 from the center of the arc, where the plasma density is highest, radially outward until the plasma density equals the background density.

The change in potential is then given by

$$\Delta V(r) = -\frac{kT_e}{e} \ln\left(\frac{n_e}{n_{e0}}\right). \quad (\text{eqn. 3.10})$$

In this ring of reduced potential, electrons in the tail of the Maxwellian distribution can cross the sheath more easily and thus a higher return current flow from the plasma to the wall results. This current flow closes the current loop of the unipolar arc. The concepts of the Schwirzke-Taylor model are illustrated in Figure 3.3.

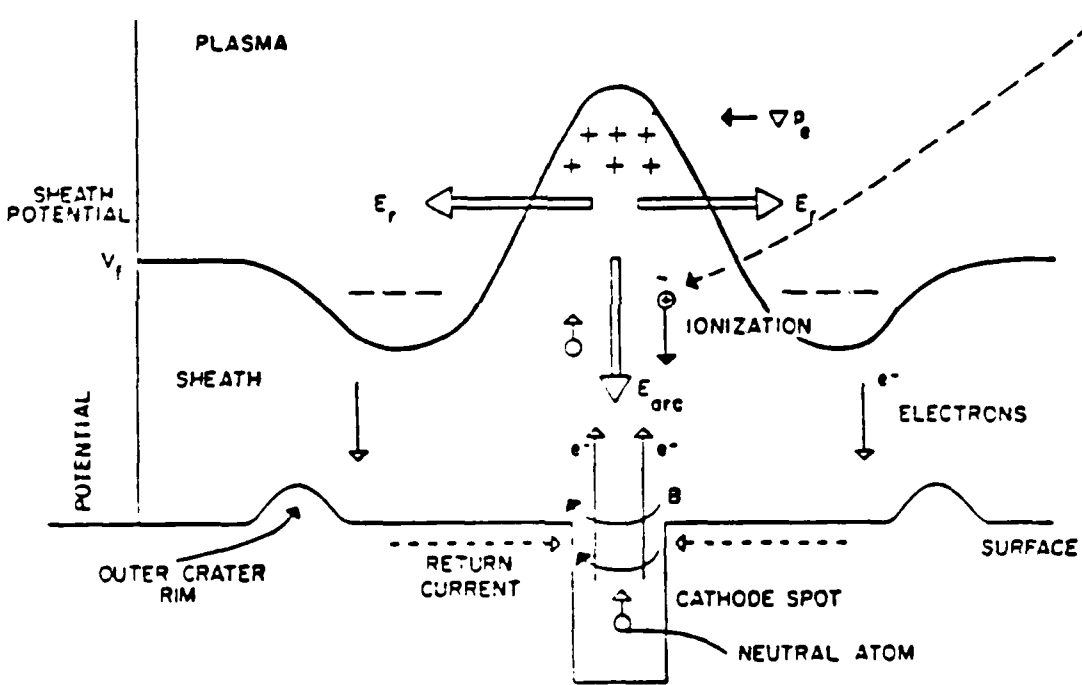


Figure 3.3 Schwirzke-Taylor Unipolar Arc Model

If equation 3.10 is set equal to the floating sheath potential, equation 3.5, the ratio of the electron density in the plasma above the spot to the background plasma density which reduces the sheath potential to zero can be determined as

$$\frac{n_e}{n_{e0}} = \sqrt{\frac{M}{2\pi m}}. \quad (\text{eqn. 3.11})$$

Equation 3.3 and equation 3.11 can be used to calculate the maximum area necessary to support a given unipolar arc return current. By setting the current equal to the current derived for the Robson-Thoneman model, equation 3.1, the ratio of the return current areas required by each model can be compared. The result of the comparison gives

$$\frac{A_{R-T}}{A_{S-T}} = \sqrt{\frac{M}{2\pi m}} \left\{ \exp\left(-\frac{eV_c}{kT_e}\right) - \sqrt{\frac{2\pi m}{M}} \right\}^{-1} > \sqrt{\frac{M}{2\pi m}} \quad (\text{eqn. 3.12})$$

where A_{R-T} and A_{S-T} are the areas required by the Robson-Thoneman model and Schwirzke-Taylor model respectively. As an example, for copper with a cathode fall potential of 15 volts and a plasma temperature of 4 eV the area ratio is 8.43×10^3 . Therefore, for a 100 ampere arc the area required by the Schwirzke-Taylor model is only $1.37 \times 10^{-2} \text{ cm}^2$, or for a circular area the radius required is only $6.59 \times 10^{-2} \text{ cm}$.

IV. CATHODE SPOTS

A. TYPES OF CATHODE SPOTS

A cathode spot is a small, luminous region on the cathode, where a localized transfer of current occurs between the cathode and a plasma in an arc discharge. The type of arc discharge can be either bipolar or unipolar, however in all cases a cathode spot is present. In addition, the spots are associated with the erosion of the cathode and therefore, are also localized centers for the transfer of material from the cathode into the plasma. This has been evidenced by the formation of craters on the surface of the cathode.

It has been possible over many observations to distinguish between two different types of cathode spots [Ref. 14]. The first type, or type I spots, are characterized as rapidly moving spots with speeds of approximately 10^4 cm/s across the surface of the cathode and with relatively low erosion from the surface. The type II spots, on the other hand, have speeds of approximately 10^2 cm/s and have much greater erosion from the surface. The type II spot also has a tendency to group together and form clusters. The mechanism of erosion for the type I spot is believed to be due to non-thermal means, such as explosions of whiskers or microinhomogenieties on the cathode surface. The erosion mechanism for the type II spot is believed

to be due to thermal evaporation.

B. THEORY OF STATIONARY CATHODE SPOTS

The theoretical modeling of cathode spots has progressed over the last 100 years, but up until the present time there has been no satisfactory understanding of the processes occurring within the spot. The difficulty occurs due to the diverse phenomena, which in themselves are extremely complicated to describe mathematically, that take place within the small cathode-plasma region known as a cathode spot. A detailed analysis would require an extensive use of the kinetic theories of Plasma Physics, Solid State Physics, Physics of High Temperature Phenomena, and Gas Dynamics. In order to avoid some of the complications the majority of models developed for the cathode spot are stationary, and therefore are unable to explain the initiation, motion, and disappearance of the cathode spot [Refs. 12 and 15].

The energy balance method developed by Lee and Greenwood [Ref. 16] has been the basis of the majority of stationary models including those proposed by Kulyapin [Ref. 17], Kubono [Ref. 18], Beilis [Ref. 19], and Moizhes and Nemchinskii [Refs. 20, 21, 22, and 23]. The latter work by Moizhes and Nemchinskii are the basis for the model developed in this paper. The cathode spot is divided into three regions as illustrated in Figure 4.1.

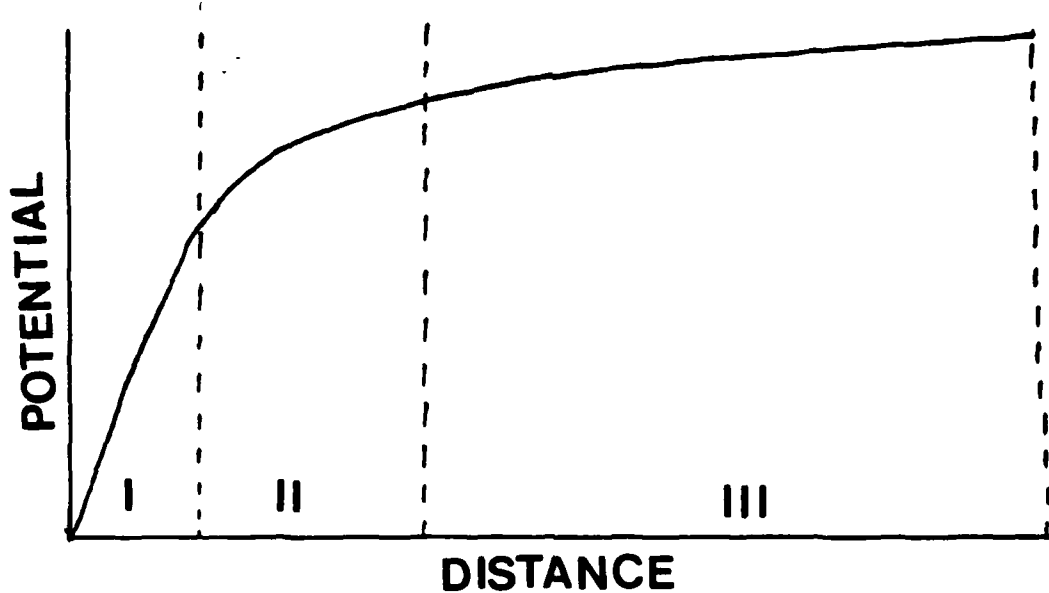


Figure 4.1 Model of the Cathode-Plasma Region

Region I, referred to as the Langmuir region, is a thin space charge sheath over which the cathode potential drop, V_k , occurs. It is in this region that the electrons emitted by the cathode are accelerated into the plasma and where the ions produced in the generation region are accelerated towards the cathode. Region II, referred to as the generation region or Knudsen Region, is where the neutral atoms evaporated from the cathode are ionized. Region III is an expanding channel or transition region over which the highly dense current channel in regions I and II expands out into the bulk plasma.

1 Fundamental Equations

In developing a theoretical model of a cathode spot, one of the first decisions that must be made is the electron emission mechanism. In general most models use a combination of thermal and field equations that are expressed as

$$j_e = f(T_k, F) \quad (\text{eqn. 4.1})$$

where j_e is the electron current density, T_k is the cathode temperature, and F is the electric field at the cathode surface. In actual use, expressions such as equation 2.41, 2.45, or 2.56 are used. The particular equation used depends on the applicability under the given conditions. The electric field at the cathode surface is determined using MacKeown's Equation, equation 2.36.

An energy balance must exist in the plasma region above the cathode spot and can be described by equation 4.2.

$$\frac{j_e}{e}(eV_k + 2kT_k) = \frac{j_i}{e}(E_i + 2kT_i) + \beta \frac{kT_p}{e}(j_e + j_i). \quad (\text{eqn. 4.2})$$

Energy is brought into the region by the electrons emitted from the cathode and consists of the thermal energy and the energy gained as the electrons were accelerated through the cathode potential drop. Energy is removed from the region by ions flowing back to the cathode. This energy loss consists of the ionization energy and the thermal energy of the ions. A further loss occurs from both ions and electrons that leave the region and pass into the bulk plasma and is described by the Peltier

heat flux βkT_e . In a plasma, in which Coulomb collisions are the predominant scattering process, the energy transfer coefficient, β , is approximately equal to 3.21. It should be noted that electrons in the plasma, also, can leave the region towards the cathode, but only if energetic enough to over come the cathode potential drop, V_k . This reverse electron current can be approximated by

$$j_{rev} = \frac{e\eta a P}{\sqrt{2\pi k T_p}} \exp\left(-\frac{eV_k}{k T_p}\right). \quad (\text{eqn. 4.3})$$

For low plasma temperatures and high cathode potential drops the reverse electron current density is much less than the ion current density and can therefore be neglected in this model.

An energy balance at the cathode surface must also exist and can be described by equation 4.4.

$$4KRT_k = \pi R^2 \left[\frac{j_i}{e} (E_i + 2kT_p + eV_k - \phi) - \frac{j_e}{e} (\phi + 2kT_k) - gE_{vap} \right]. \quad (\text{eqn. 4.4})$$

The predominant loss mechanisms considered are heat conduction, emissive cooling, and evaporation. The primary energy source considered is ion bombardment of the cathode surface. The ions bring to the surface thermal energy, ionization energy, and energy gained while being accelerated by the cathode potential drop. Energy is released, approximately equal to the work function, when ions and electrons recombine at the surface. The electrons emitted by the surface remove thermal energy and an

energy approximately equal to the work function. In addition, neutral atoms, evaporating from the surface, remove energy equivalent to the heat of vaporization. Heat conduction from the cathode spot is based on a circular spot of radius R at a constant temperature T_k and where κ is the thermal conductivity of the cathode. The work function to be used in equation 4.4 is corrected for the Schottky effect and is given by

$$\phi = \phi_0 - \sqrt{\frac{e^3 F}{4\pi\epsilon_0}}. \quad (\text{eqn. 4.5})$$

The total current flow in the arc is given by

$$I = \pi R^2 (j_e + j_i). \quad (\text{eqn. 4.6})$$

A fraction of the neutral atoms evaporated from the cathode will return to the cathode. The return coefficient can be determined from equation 4.7 which is based on a Monte Carlo calculation performed by Nemchinskii [Ref. 24].

$$\eta = \left(\frac{8}{3} + \alpha - \sqrt{\frac{5\pi T_e}{6T_s}} \right) \left(\frac{8}{3} + \alpha + \sqrt{\frac{5\pi}{6}} \right)^{-1}. \quad (\text{eqn. 4.6})$$

The ion current density is determined from

$$j_i = \frac{1}{4} e n_i \bar{u} \quad (\text{eqn. 4.8})$$

where

$$n_i = \frac{P a \eta}{k T_s} \quad (\text{eqn. 4.9})$$

and

$$\bar{u} = \sqrt{\frac{8kT_e}{\pi M}}. \quad (\text{eqn. 4.10})$$

Substituting equations 4.9 and 4.10 into equation 4.8 gives the ion current density as

$$j_i = \frac{eP}{\sqrt{2\pi M k T_e}} \eta \alpha(T_e) \quad (\text{eqn. 4.11})$$

where P is the vapor pressure of the cathode material and α is the degree of ionization. The degree of ionization is determined from Saha's Equation which is expressed as

$$\alpha = \left\{ \sqrt{1 + \frac{P}{k T_e} \left(\frac{2\pi h^2}{M k T_e} \right)^{\frac{3}{2}}} \exp\left(\frac{E_i}{k T_e}\right) \right\}^{-1}. \quad (\text{eqn. 4.12})$$

The erosion rate of neutral atoms is given by

$$g = \frac{P}{\sqrt{2\pi M k T_e}} (1 - \eta). \quad (\text{eqn. 4.13})$$

The potential drop inside the quasineutral plasma of the transition region is given by

$$U = \left[\left(\frac{I}{2\pi\sigma R} \right) \left(\frac{eg}{j} \right) (1+z) - \beta K T_e \right] \left[1 + \left(\frac{eg}{j} \right) (1+z) \right]^{-1} \quad (\text{eqn. 4.14})$$

where z is the average charge of the ions in the region, j is the total current density given by

$$j = j_i + j_e \quad (\text{eqn. 4.15})$$

and σ is the electric conductivity given by

$$\sigma = \frac{1.53 \times 10^{-2}}{\ln A} T^{\frac{3}{2}} \quad (\text{eqn. 4.16})$$

where the Coulomb Logarithm is approximated as

$$\ln A = 23 - \ln \left(\frac{1}{T^{\frac{3}{2}}} \sqrt{\frac{P}{k}} \right). \quad (\text{eqn. 4.17})$$

The total potential drop across the arc is given by

$$V_{arc} = V_t + U. \quad (\text{eqn. 4.18})$$

2. Method of Solution

The system of equations presented in the previous section is not closed. Therefore, more information is required in order to solve the system. This will be accomplished here using the Steenbeck Minimum Principle [Refs. 25 and 26]. Simply stated this requires that the total potential drop across the arc must be a minimum for a stationary arc to exist. Given an arc current and cathode temperature the system of equations is solved for the cathode potential drop, plasma temperature, ion current density, electron current density, erosion rate, potential drop in the transition region, and total arc potential drop. The cathode temperature that defines the stationary cathode spot, for the given arc current, is that cathode temperature that minimizes the total potential drop. If a minimum total arc potential can not be found for a given arc current, then a stable arc can not exist for this current.

The first step in the solution is to determine the plasma temperature, T_p , and cathode drop, V_k . To accomplish this a guess is made for the plasma temperature. The partial pressure of the cathode material is determined using [Ref. 27]

$$\log P = \frac{A}{T_p} + B \log T_p + C T_p + D \quad (\text{eqn. 4.19})$$

where for copper $A = -1752 \times 10^4$, $B = -1.21$, $C = 0$, and $D = 13.21$. The degree of ionization is determined using equation 4.12 and the return coefficient is determined using equation 4.6. The ion current density can now be determined using equation 4.11. Experimentally, it has been observed that the cathode drop is approximately 15 volts, so this will be used as a first approximation in order to determine the electric field at the cathode surface using equation 2.36. The Schottky corrected work function is determined using equation 4.5 and the electron current density is determined using equation 4.1. The spot radius can now be determined using equation 4.6. The erosion rate is determined from equation 4.13. Equation 4.2 and 4.4 are each solved separately for the cathode potential which gives

$$V_{k1} = \frac{1}{e} \left\{ \frac{j_t}{j_e} (E_i + 2kT_p) + \beta kT_p \left(1 + \frac{j_t}{j_e} \right) - 2kT_k \right\} \quad (\text{eqn. 4.20})$$

and

$$V_{k2} = \frac{4u}{\pi R j_i} T_k + \frac{1}{e} \left\{ \frac{j_o}{j_i} (\phi + 2kT_k) - E_i - 2kT_p + \phi \right\} + \frac{g}{j_i} E_{vap}.$$

(eqn. 4.21)

The potential is then determined using both equation 4.20 and 4.21. The results are compared and the plasma temperature is then adjusted. This procedure is then repeated until the potentials determined from both equations are in agreement. The conductivity is determined using equation 4.16 and 4.17. The potential drop in the transition region is then determined using equation 4.14. Finally, the total arc potential is determined from equation 4.18. Appendix J is a Fortran program, which uses the method described above, to calculate the cathode spot parameters.

V. COMPARISON OF THEORY AND EXPERIMENTAL DATA

The Fortran program listed in Appendix J was used to calculate the parameters of the cathode spot for arc currents of 100, 150, 175, 200, 300 and 400 Amperes. The program required knowledge of several material parameters which are specified in Table 1.

TABLE 1
CATHODE SPOT MODEL CONSTANTS

Constant	Value
Material	Copper
Ion Mass (gr/mole)	63.54
Heat of Vaporization (kilojoules)	300.3
Ionization Energy (eV)	7.726
Work Function (eV)	4.4
Thermal Conductivity (W/m-K)	40

Figure 5.1 illustrates the variation of the total arc potential with cathode temperature for different arc currents. The cathode temperature for a stable cathode spot, and thus the parameters of the cathode spot, is determined from the minimum of the total arc potential. It can be seen from Figure 5.1 that a stable arc does not occur for arc currents below 200 Amperes.

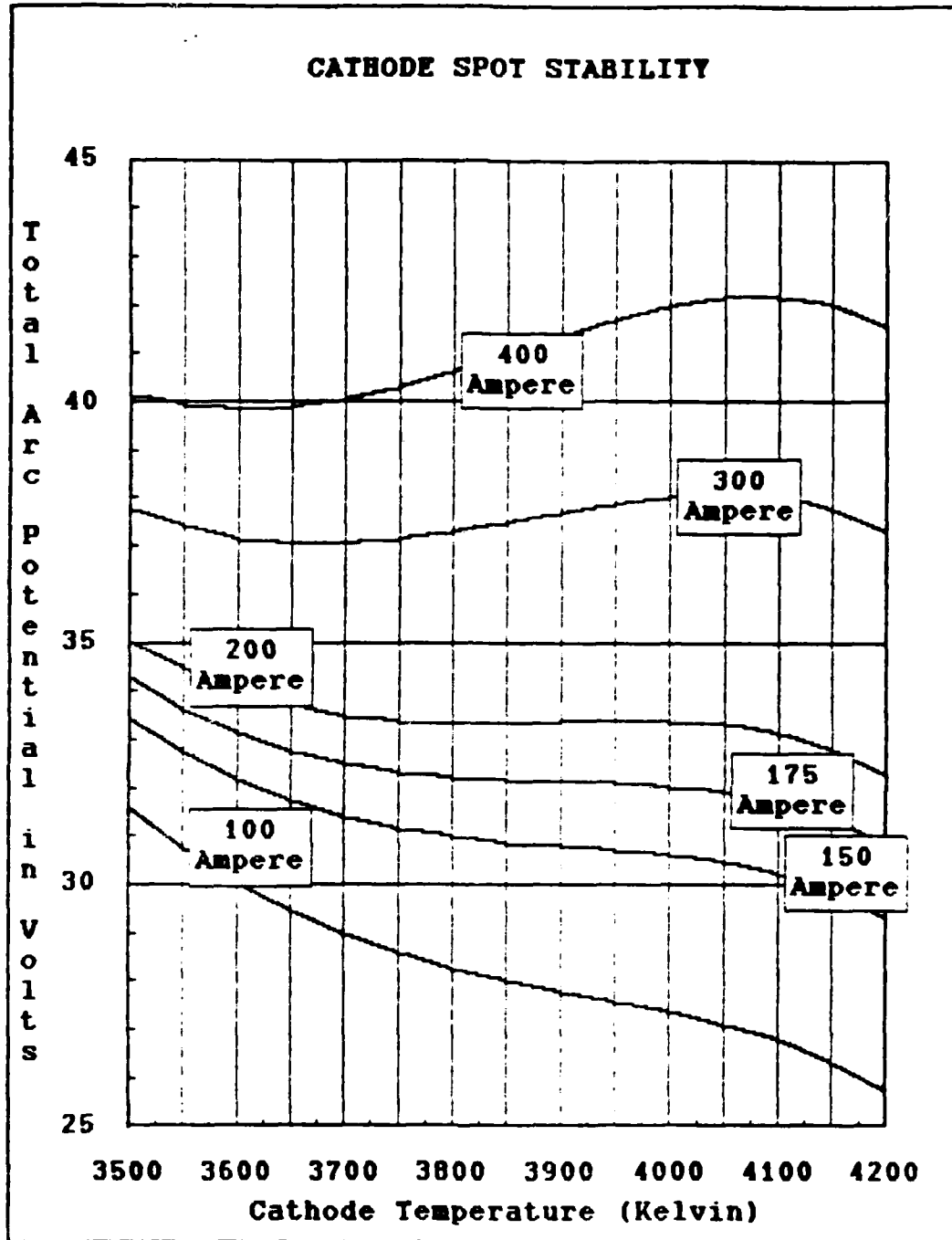


Figure 5.1 Cathode Spot Stability

The results of the calculations are listed in Table 2 through 7 for arc currents of 100, 150, 175, 200, 300, and 400 Amperes respectively. In addition Figures 5.2 through 5.7 illustrate the variation of the cathode potential transition region potential and total arc potential for each arc current.

The cathode spot parameters for stable arc currents of 200, 300, and 400 Amperes are summarized in Table 8. The results are in general order of magnitude, agreement with experimental data [Ref. 23], however stability has been indicated at arc currents between 100 and 200 Amperes. This discrepancy occurs since the material constants listed in Table 1 are not really constants at these temperatures. A more detailed comparison is not warranted, since the published experimental data for the cathode spot parameters vary widely. Confirmation of the models of the cathode phenomena is greatly limited by this lack of consistent experimental results.

TABLE 2
CATHODE SPOT PARAMETERS FOR A 100 AMPERE ARC ON A
COPPER CATHODE

Cathode Temperature (Kelvin)	Plasma Temperature (eV)	Cathode Potential (Volts)	Transition Potential (Volts)	Total Arc Potential (Volts)
3500	1.49	22.89	8.72	31.61
3550	1.54	21.54	9.21	30.75
3600	1.59	20.34	9.70	30.04
3650	1.65	19.27	10.18	29.45
3700	1.70	18.32	10.65	28.97
3750	1.76	17.49	11.10	28.59
3800	1.82	16.75	11.53	28.28
3850	1.89	16.10	11.92	28.02
3900	1.96	15.54	12.26	27.80
3950	2.03	15.06	12.53	27.59
4000	2.11	14.66	12.71	27.37
4050	2.20	14.34	12.78	27.11
4100	2.29	14.09	12.70	26.79
4150	2.39	13.91	12.44	26.35
4200	2.51	13.82	11.94	25.76
Cathode Temperature (Kelvin)	Partial Pressure (atm.)	Degree of Ionization	Return Coefficient	Spot Radius (10^{-4} m)
3500	10.9	0.1625	0.4726	4.807
3550	12.6	0.1712	0.4751	4.258
3600	14.5	0.1803	0.4777	3.777
3650	16.6	0.1897	0.4804	3.354
3700	19.0	0.1996	0.4831	2.981
3750	21.6	0.2101	0.4859	2.652
3800	24.5	0.2213	0.4888	2.360
3850	27.6	0.2332	0.4918	2.100
3900	31.1	0.2461	0.4950	1.869
3950	34.9	0.2602	0.4983	1.663
4000	39.1	0.2758	0.5018	1.478
4050	43.6	0.2931	0.5057	1.312
4100	48.5	0.3125	0.5098	1.163
4150	53.8	0.3348	0.5144	1.028
4200	59.6	0.3606	0.5195	0.905

TABLE 2 (CONTINUED)
CATHODE SPOT PARAMETERS FOR A 100 AMPERE ARC ON A
COPPER CATHODE

Cathode Temperature (Kelvin)	Electric Field (10^6 V/m)	Electron Current Density (10^6 A/m 2)	Ion Current Density (10^6 A/m 2)	Total Current Density (10^6 A/m 2)
3500	3.055	0.625	0.753	1.378
3550	3.318	0.841	0.915	1.756
3600	3.598	1.124	1.108	2.232
3650	3.896	1.495	1.335	2.830
3700	4.214	1.980	1.602	3.582
3750	4.555	2.610	1.917	4.527
3800	4.921	3.430	2.288	5.717
3850	5.315	4.493	2.723	7.216
3900	5.741	5.874	3.236	9.110
3950	6.205	7.670	3.841	11.51
4000	6.712	10.01	4.559	14.57
4050	7.270	13.07	5.412	18.49
4100	7.889	17.11	6.435	23.54
4150	8.583	22.47	7.670	30.14
4200	9.368	29.69	9.177	38.87
Cathode Temperature (Kelvin)	Ion/Total Current Density Ratio	Coulomb Logarithm	Conductivity (mho/m)	Erosion Rate (10^{27} atoms/m 2 -s)
3500	.5462	10.5	3309	3.226
3550	.5212	10.5	3489	3.686
3600	.4963	10.5	3679	4.193
3650	.4717	10.4	3879	4.750
3700	.4474	10.4	4091	5.360
3750	.4235	10.4	4315	6.025
3800	.4001	10.4	4553	6.748
3850	.3773	10.3	4808	7.530
3900	.3552	10.3	5082	8.372
3950	.3337	10.3	5378	9.276
4000	.3129	10.3	5701	10.24
4050	.2928	10.3	6057	11.27
4100	.2733	10.3	6452	12.36
4150	.2545	10.3	6898	13.50
4200	.2361	10.3	7409	14.69

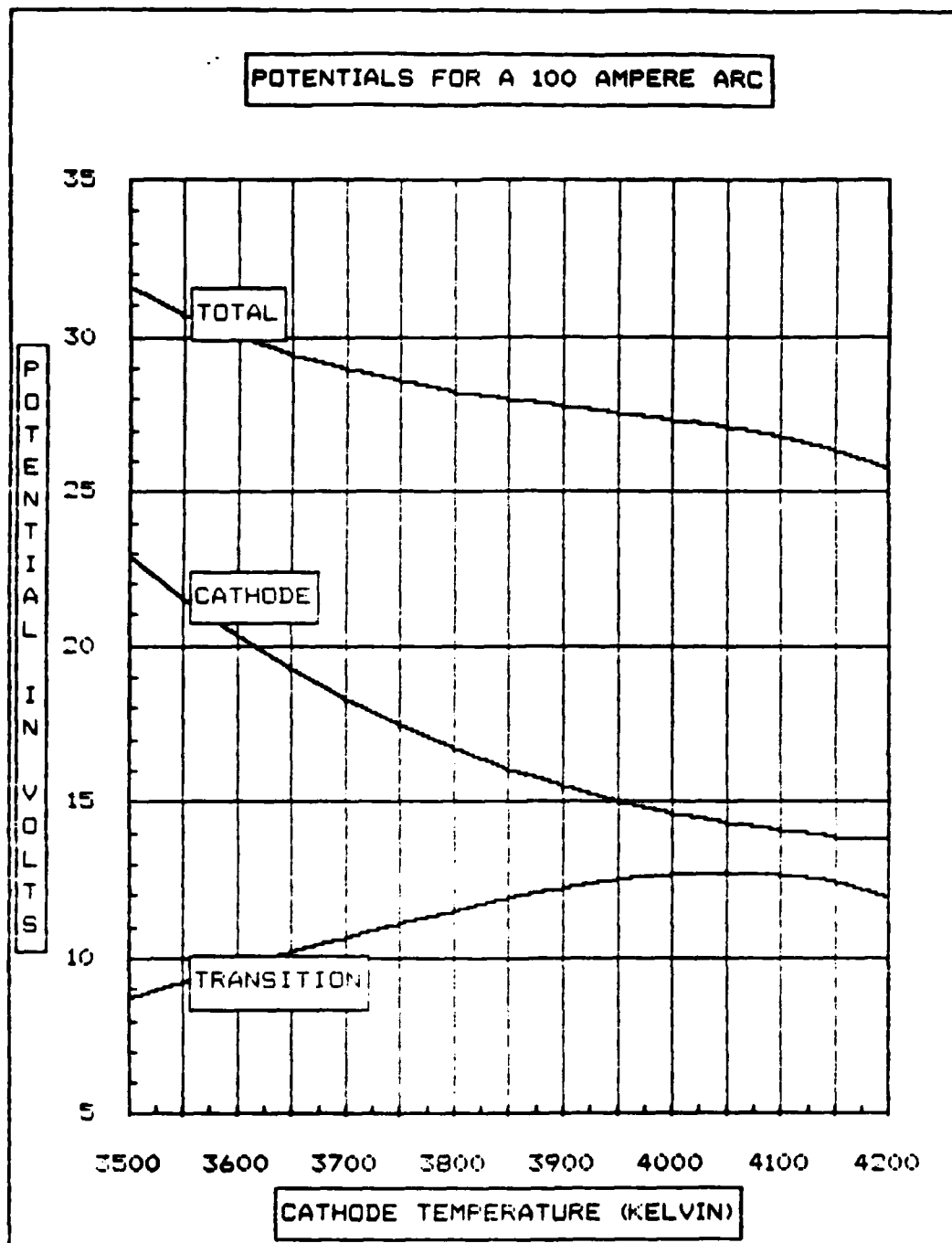


Figure 5.2 Potentials for a 100 Ampere Arc

TABLE 3
CATHODE SPOT PARAMETERS FOR A 150 AMPERE ARC ON A
COPPER CATHODE

Cathode Temperature (Kelvin)	Plasma Temperature (eV)	Cathode Potential (Volts)	Transition Potential (Volts)	Total Arc Potential (Volts)
3500	1.48	22.66	10.79	33.45
3550	1.53	21.33	11.41	32.74
3600	1.58	20.15	12.03	32.18
3650	1.64	19.09	12.65	31.74
3700	1.69	18.16	13.25	31.41
3750	1.75	17.33	13.84	31.17
3800	1.81	16.60	14.41	31.01
3850	1.88	15.96	14.93	30.89
3900	1.94	15.41	15.40	30.81
3950	2.02	14.94	15.79	30.73
4000	2.09	14.54	16.08	30.63
4050	2.18	14.22	16.25	30.47
4100	2.27	13.97	16.26	30.23
4150	2.37	13.80	16.06	29.85
4200	2.49	13.70	15.59	29.30
Cathode Temperature (Kelvin)	Partial Pressure (atm.)	Degree of Ionization	Return Coefficient	Spot Radius (10^{-4} m)
3500	10.9	0.1589	0.4716	5.948
3550	12.6	0.1674	0.4742	5.269
3600	14.5	0.1763	0.4768	4.674
3650	16.6	0.1855	0.4794	4.151
3700	19.0	0.1952	0.4821	3.690
3750	21.6	0.2055	0.4849	3.282
3800	24.5	0.2164	0.4877	2.921
3850	27.6	0.2281	0.4907	2.600
3900	31.1	0.2407	0.4938	2.315
3950	34.9	0.2544	0.4971	2.060
4000	39.1	0.2696	0.5006	1.831
4050	43.6	0.2864	0.5044	1.626
4100	48.5	0.3054	0.5084	1.442
4150	53.8	0.3271	0.5129	1.275
4200	59.6	0.3522	0.5180	1.123

TABLE 3 (CONTINUED)
CATHODE SPOT PARAMETERS FOR A 150 AMPERE ARC ON A
COPPER CATHODE

Cathode Temperature (Kelvin)	Electric Field (10^6 V/m)	Electron Current Density (10^6 A/m 2)	Ion Current Density (10^6 A/m 2)	Total Current Density (10^6 A/m 2)
3500	3.011	0.615	0.735	1.349
3550	3.270	0.827	0.893	1.720
3600	3.546	1.105	1.081	2.185
3650	3.840	1.469	1.303	2.771
3700	4.153	1.944	1.564	3.508
3750	4.489	2.562	1.871	4.433
3800	4.850	3.364	2.232	5.596
3850	5.238	4.405	2.657	7.061
3900	5.658	5.755	3.157	8.912
3950	6.115	7.509	3.747	11.26
4000	6.614	9.792	4.445	14.24
4050	7.163	12.78	5.277	18.06
4100	7.772	16.71	6.272	22.98
4150	8.454	21.92	7.473	29.39
4200	9.225	28.92	8.937	37.86
Cathode Temperature (Kelvin)	Ion/Total Current Density Ratio	Coulomb Logarithm	Conductivity (mho/m)	Erosion Rate (10^{27} atoms/m 2 -s)
3500	0.5443	10.5	3279	3.232
3550	0.5194	10.5	3458	3.692
3600	0.4946	10.5	3645	4.200
3650	0.4700	10.4	3842	4.759
3700	0.4458	10.4	4051	5.371
3750	0.4221	10.4	4272	6.038
3800	0.3989	10.4	4506	6.762
3850	0.3762	10.3	4757	7.547
3900	0.3542	10.3	5027	8.392
3950	0.3329	10.3	5318	9.299
4000	0.3122	10.3	5636	10.27
4050	0.2923	10.3	5985	11.30
4100	0.2729	10.3	6372	12.39
4150	0.2542	10.3	6808	13.54
4200	0.2361	10.3	7307	14.74

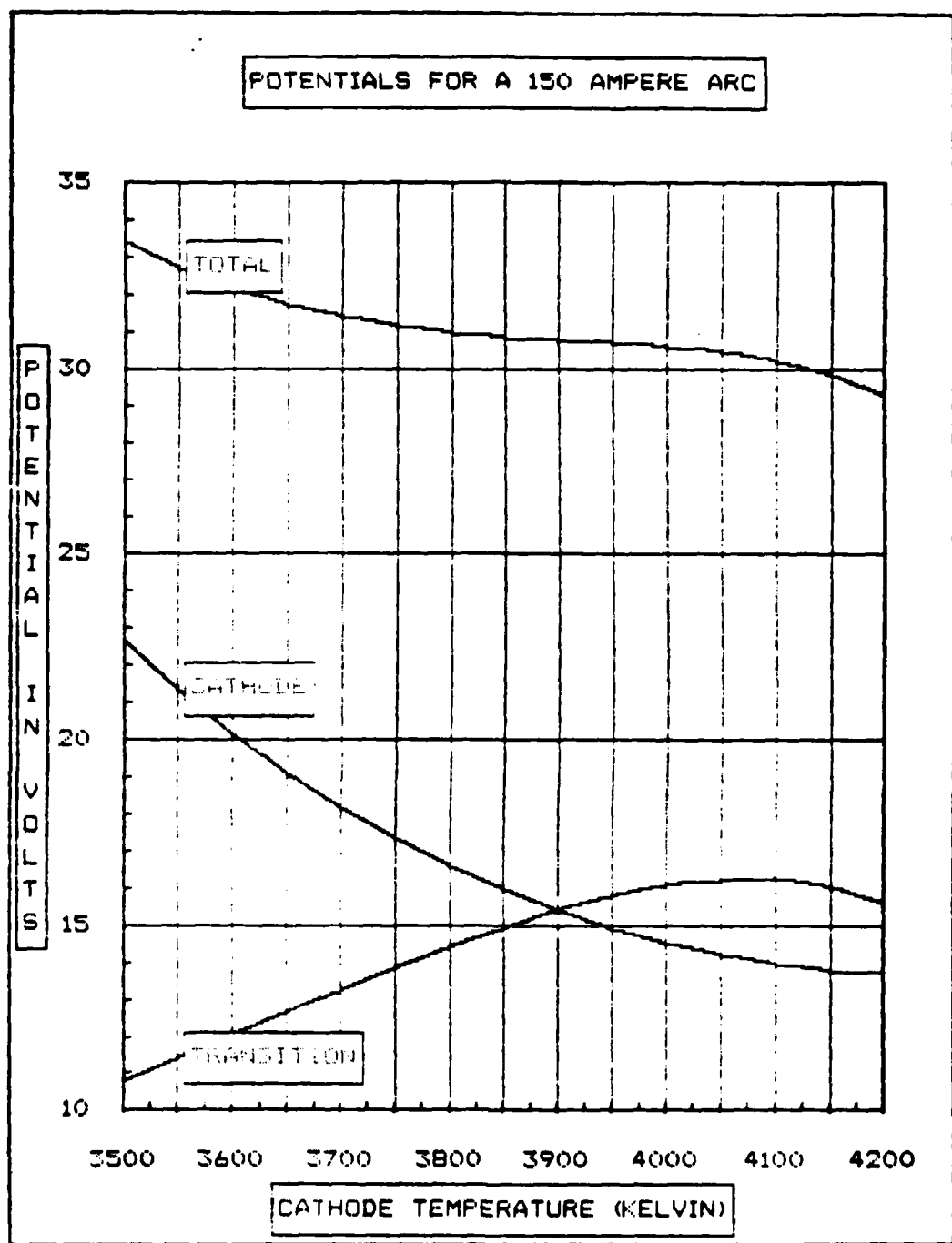


Figure 5.3 Potentials for a 150 Ampere Arc

TABLE 4
CATHODE SPOT PARAMETERS FOR A 175 AMPERE ARC ON A
COPPER CATHODE

Cathode Temperature (Kelvin)	Plasma Temperature (eV)	Cathode Potential (Volts)	Transition Potential (Volts)	Total Arc Potential (Volts)
3500	1.48	22.61	11.69	34.29
3550	1.53	21.26	12.37	33.63
3600	1.58	20.08	13.04	33.13
3650	1.63	19.04	13.72	32.76
3700	1.69	18.10	14.39	32.49
3750	1.75	17.28	15.04	32.32
3800	1.81	16.55	15.66	32.21
3850	1.87	15.92	16.24	32.16
3900	1.94	15.37	16.76	32.13
3950	2.01	14.90	17.21	32.11
4000	2.09	14.50	17.55	32.05
4050	2.17	14.18	17.76	31.95
4100	2.26	13.93	17.80	31.74
4150	2.37	13.76	17.63	31.39
4200	2.48	13.66	17.18	30.84
Cathode Temperature (Kelvin)	Partial Pressure (atm.)	Degree of Ionization	Return Coefficient	Spot Radius (10^{-4} m)
3500	10.9	0.1578	0.4714	6.452
3550	12.6	0.1662	0.4739	5.711
3600	14.5	0.1750	0.4765	5.066
3650	16.6	0.1842	0.4791	4.499
3700	19.0	0.1938	0.4818	3.999
3750	21.6	0.2040	0.4845	3.556
3800	24.5	0.2148	0.4874	3.166
3850	27.6	0.2264	0.4903	2.819
3900	31.1	0.2389	0.4934	2.509
3950	34.9	0.2525	0.4967	2.233
4000	39.1	0.2676	0.5002	1.986
4050	43.6	0.2843	0.5039	1.763
4100	48.5	0.3031	0.5080	1.563
4150	53.8	0.3246	0.5125	1.382
4200	59.6	0.3495	0.5175	1.218

TABLE 4 (CONTINUED)
CATHODE SPOT PARAMETERS FOR A 175 AMPERE ARC ON A
COPPER CATHODE

Cathode Temperature (Kelvin)	Electric Field (10^6 V/m)	Electron Current Density (10^6 A/m 2)	Ion Current Density (10^6 A/m 2)	Total Current Density (10^6 A/m 2)
3500	2.986	0.609	0.729	1.338
3550	3.254	0.822	0.886	1.708
3600	3.528	1.098	1.072	2.171
3650	3.821	1.460	1.292	2.752
3700	4.133	1.932	1.551	3.483
3750	4.468	2.546	1.856	4.402
3800	4.827	3.342	2.214	5.557
3850	5.213	4.376	2.635	7.011
3900	5.631	5.716	3.131	8.847
3950	6.085	7.456	3.716	11.17
4000	6.581	9.722	4.408	14.13
4050	7.128	12.68	5.232	17.91
4100	7.734	16.58	6.218	22.79
4150	8.412	21.74	7.408	29.15
4200	9.178	28.67	8.859	37.53
Cathode Temperature (Kelvin)	Ion/Total Current Density Ratio	Coulomb Logarithm	Conductivity (mho/m)	Erosion Rate (10^{27} atoms/m 2 -s)
3500	0.5448	10.5	3270	3.233
3550	0.5188	10.5	3447	3.694
3600	0.4940	10.5	3634	4.203
3650	0.4695	10.4	3830	4.762
3700	0.4453	10.4	4038	5.374
3750	0.4216	10.4	4258	6.042
3800	0.3984	10.4	4491	6.767
3850	0.3758	10.3	4741	7.552
3900	0.3539	10.3	5009	8.398
3950	0.3326	10.3	5299	9.306
4000	0.3120	10.3	5614	10.28
4050	0.2921	10.3	5961	11.31
4100	0.2728	10.3	6346	12.40
4150	0.2542	10.3	6779	13.55
4200	0.2361	10.3	7274	14.75

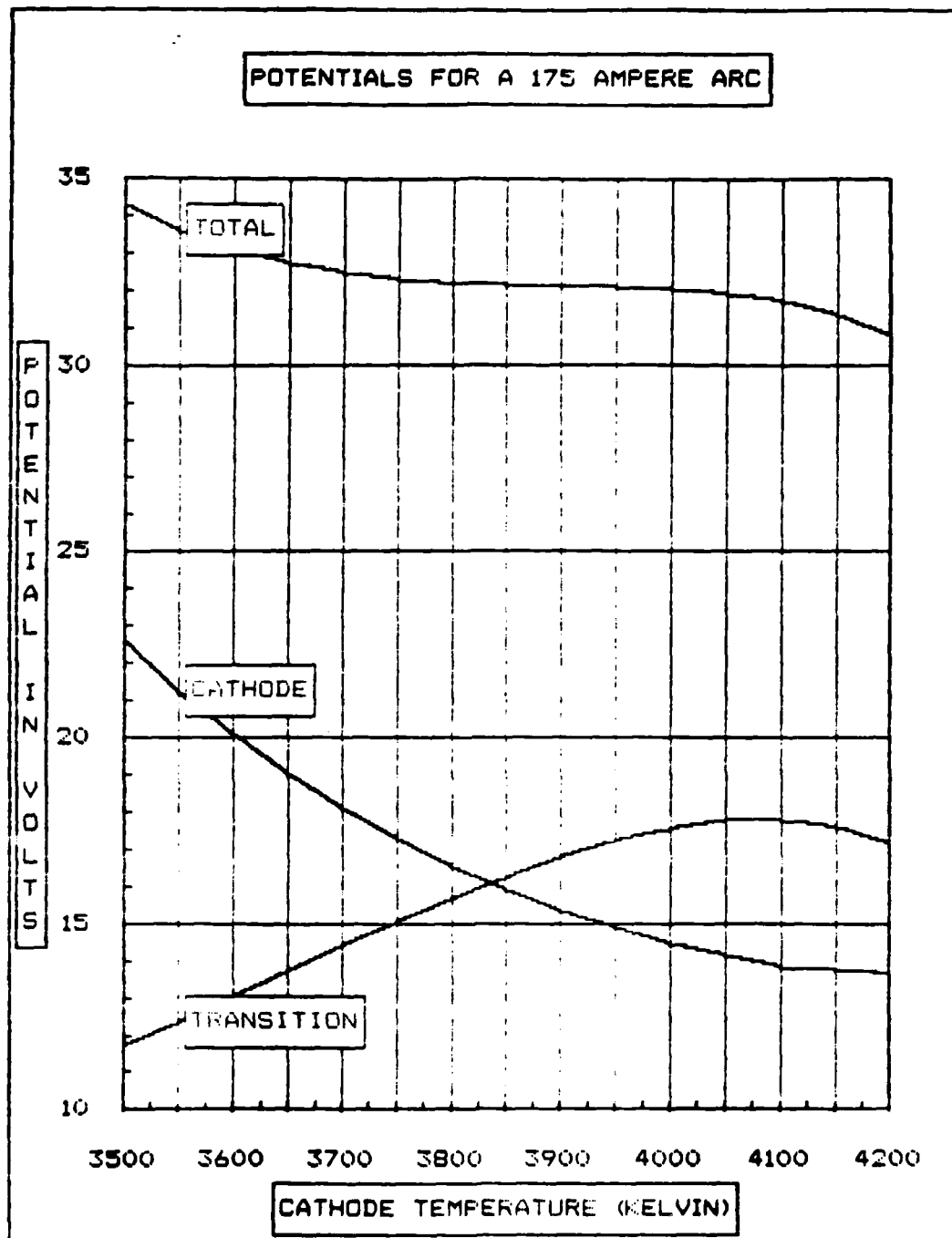


Figure 5.4 Potentials for a 175 Ampere Arc

TABLE 5
CATHODE SPOT PARAMETERS FOR A 200 AMPERE ARC ON A
COPPER CATHODE

Cathode Temperature (Kelvin)	Plasma Temperature (eV)	Cathode Potential (Volts)	Transition Potential (Volts)	Total Arc Potential (Volts)
3500	1.48	22.48	12.53	35.01
3550	1.53	21.21	13.26	34.47
3600	1.58	20.03	13.99	34.02
3650	1.63	18.99	14.72	33.71
3700	1.69	18.06	15.44	33.50
3750	1.74	17.24	16.15	33.38
3800	1.80	16.51	16.82	33.34
3850	1.87	15.88	17.46	33.34
3900	1.94	15.33	18.03	33.37
3950	2.01	14.86	18.53	33.39
4000	2.08	14.47	18.92	33.39
4050	2.17	14.15	19.17	33.32
4100	2.26	13.90	19.24	33.15
4150	2.36	13.73	19.09	32.82
4200	2.47	13.63	18.65	32.28
Cathode Temperature (Kelvin)	Partial Pressure (atm.)	Degree of Ionization	Return Coefficient	Spot Radius (10^{-4} m)
3500	10.9	0.1575	0.4713	6.899
3550	12.6	0.1652	0.4736	6.122
3600	14.5	0.1739	0.4762	5.431
3650	16.6	0.1830	0.4788	4.823
3700	19.0	0.1926	0.4815	4.287
3750	21.6	0.2027	0.4842	3.814
3800	24.5	0.2135	0.4871	3.395
3850	27.6	0.2250	0.4900	3.022
3900	31.1	0.2374	0.4931	2.690
3950	34.9	0.2510	0.4964	2.394
4000	39.1	0.2659	0.4998	2.129
4050	43.6	0.2825	0.5036	1.891
4100	48.5	0.3012	0.5076	1.677
4150	53.8	0.3226	0.5121	1.483
4200	59.6	0.3473	0.5171	1.307

TABLE 5 (CONTINUED)
CATHODE SPOT PARAMETERS FOR A 200 AMPERE ARC ON A
COPPER CATHODE

Cathode Temperature (Kelvin)	Electric Field (10^6 V/m)	Electron Current Density (10^6 A/m 2)	Ion Current Density (10^6 A/m 2)	Total Current Density (10^6 A/m 2)
3500	2.990	0.610	0.727	1.338
3550	3.241	0.818	0.880	1.698
3600	3.515	1.093	1.065	2.159
3650	3.806	1.453	1.284	2.737
3700	4.117	1.923	1.541	3.464
3750	4.450	2.533	1.844	4.377
3800	4.808	3.326	2.199	5.525
3850	5.193	4.353	2.617	6.970
3900	5.609	5.685	3.110	8.795
3950	6.061	7.414	3.691	11.11
4000	6.556	9.665	4.379	14.04
4050	7.100	12.61	5.197	17.80
4100	7.703	16.47	6.176	22.65
4150	8.378	21.60	7.357	28.95
4200	9.141	28.47	8.797	37.27
Cathode Temperature (Kelvin)	Ion/Total Current Density Ratio	Coulomb Logarithm	Conductivity (mho/m)	Erosion Rate (10^{27} atoms/m 2 -s)
3500	0.5438	10.5	3267	3.234
3550	0.5183	10.5	3439	3.696
3600	0.4935	10.5	3625	4.205
3650	0.4690	10.4	3820	4.765
3700	0.4449	10.4	4027	5.377
3750	0.4212	10.4	4246	6.045
3800	0.3981	10.4	4479	6.771
3850	0.3755	10.3	4727	7.556
3900	0.3536	10.3	4994	8.403
3950	0.3323	10.3	5283	9.312
4000	0.3118	10.3	5597	10.28
4050	0.2919	10.3	5942	11.32
4100	0.2727	10.3	6325	12.41
4150	0.2541	10.3	6755	13.56
4200	0.2360	10.3	7247	14.77

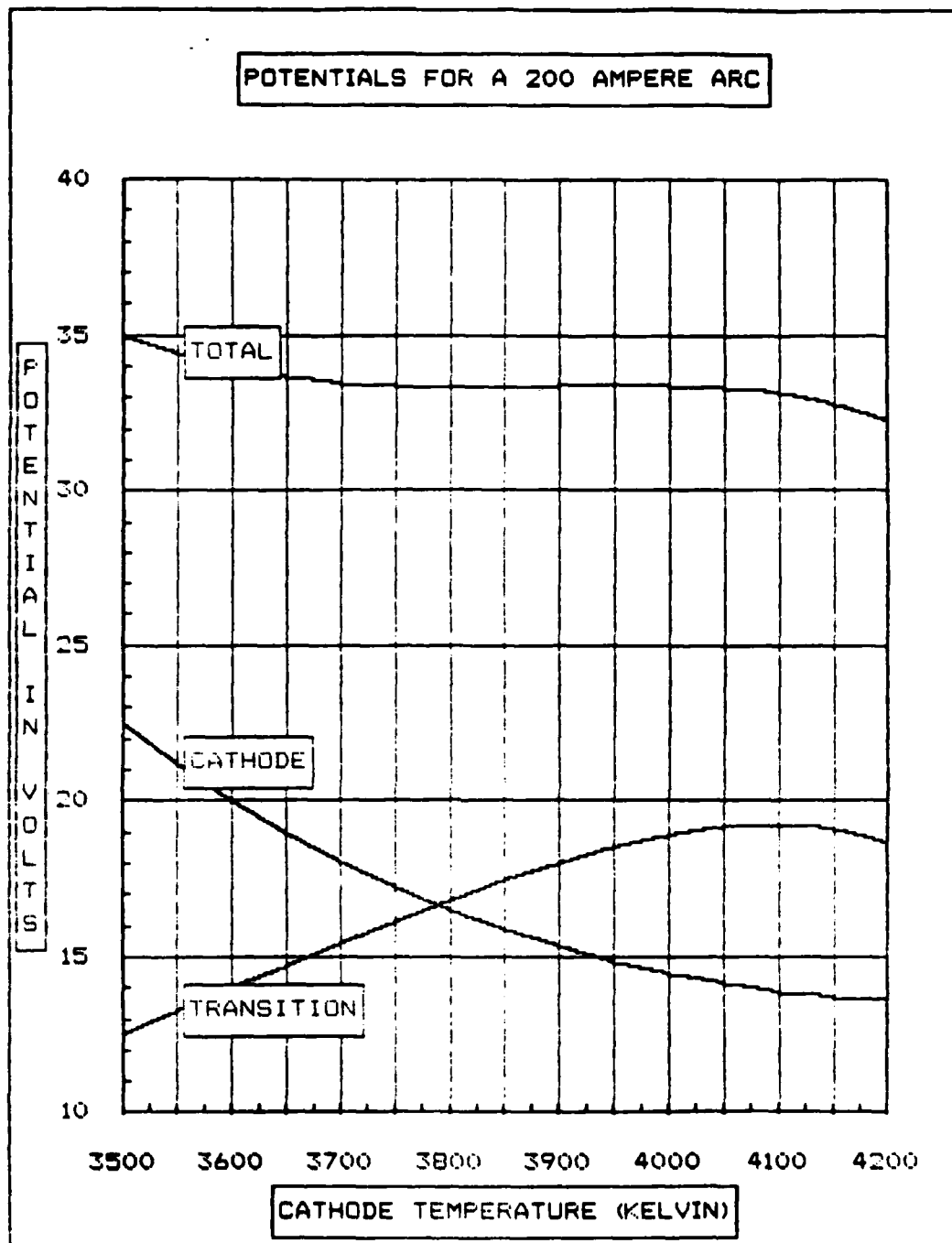


Figure 5.5 Potentials for a 200 Ampere Arc

TABLE 6
CATHODE SPOT PARAMETERS FOR A 300 AMPERE ARC ON A
COPPER CATHODE

Cathode Temperature (Kelvin)	Plasma Temperature (eV)	Cathode Potential (Volts)	Transition Potential (Volts)	Total Arc Potential (Volts)
3500	1.47	22.32	15.45	37.77
3550	1.52	21.06	16.36	37.42
3600	1.57	19.90	17.28	37.17
3650	1.62	18.86	18.20	37.06
3700	1.68	17.94	19.11	37.05
3750	1.74	17.13	20.00	37.13
3800	1.80	16.41	20.87	37.28
3850	1.86	15.78	21.69	37.47
3900	1.93	15.24	22.45	37.69
3950	2.00	14.77	23.11	37.89
4000	2.07	14.38	23.66	38.04
4050	2.15	14.07	24.04	38.11
4100	2.25	13.82	24.23	38.05
4150	2.34	13.65	24.15	37.80
4200	2.46	13.55	23.75	37.30
Cathode Temperature (Kelvin)	Partial Pressure (atm.)	Degree of Ionization	Return Coefficient	Spot Radius (10^{-4} m)
3500	10.9	0.1550	0.4706	8.513
3550	12.6	0.1626	0.4730	7.554
3600	14.5	0.1712	0.4755	6.701
3650	16.6	0.1801	0.4781	5.951
3700	19.0	0.1896	0.4808	5.290
3750	21.6	0.1995	0.4835	4.707
3800	24.5	0.2101	0.4863	4.189
3850	27.6	0.2214	0.4892	3.730
3900	31.1	0.2336	0.4923	3.321
3950	34.9	0.2470	0.4955	2.956
4000	39.1	0.2616	0.4990	2.629
4050	43.6	0.2779	0.5027	2.336
4100	48.5	0.2963	0.5067	2.071
4150	53.8	0.3172	0.5111	1.832
4200	59.6	0.3415	0.5160	1.616

TABLE 6 (CONTINUED)
CATHODE SPOT PARAMETERS FOR A 300 AMPERE ARC ON A
COPPER CATHODE

Cathode Temperature (Kelvin)	Electric Field (10^6 V/m)	Electron Current Density (10^6 A/m 2)	Ion Current Density (10^6 A/m 2)	Total Current Density (10^6 A/m 2)
3500	2.959	0.603	0.715	1.318
3550	3.207	0.808	0.865	1.673
3600	3.478	1.080	1.047	2.127
3650	3.767	1.435	1.261	2.696
3700	4.075	1.898	1.514	3.412
3750	4.404	2.500	1.811	4.311
3800	4.758	3.280	2.161	5.441
3850	5.139	4.292	2.572	6.863
3900	5.551	5.603	3.055	8.658
3950	5.998	7.304	3.625	10.93
4000	6.487	9.516	4.300	13.82
4050	7.025	12.40	5.103	17.51
4100	7.621	16.20	6.063	22.26
4150	8.287	21.22	7.221	28.44
4200	9.040	27.95	8.632	36.58
Cathode Temperature (Kelvin)	Ion/Total Current Density Ratio	Coulomb Logarithm	Conductivity (mho/m)	Erosion Rate (10^{27} atoms/m 2 -s)
3500	0.5423	10.5	3246	3.238
3550	0.5169	10.5	3416	3.701
3600	0.4922	10.5	3600	4.211
3650	0.4678	10.4	3794	4.771
3700	0.4438	10.4	3999	5.385
3750	0.4202	10.4	4216	6.054
3800	0.3971	10.4	4446	6.781
3850	0.3747	10.3	4692	7.568
3900	0.3528	10.3	4956	8.417
3950	0.3317	10.3	5241	9.328
4000	0.3113	10.3	5551	10.30
4050	0.2915	10.3	5891	11.34
4100	0.2724	10.3	6269	12.44
4150	0.2539	10.3	6693	13.59
4200	0.2360	10.3	7176	14.80

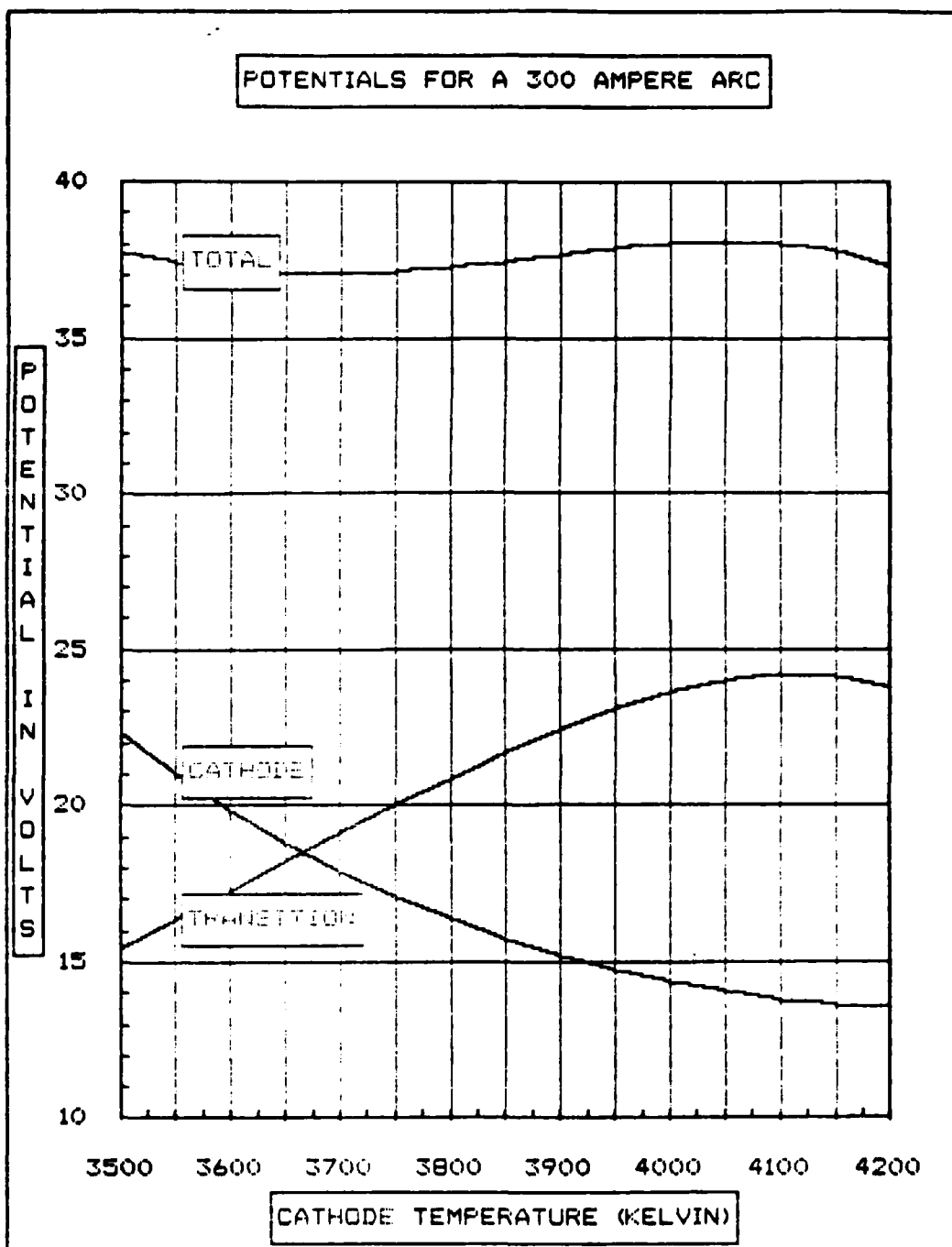


Figure 5.6 Potentials for a 300 Ampere Arc

TABLE 7
CATHODE SPOT PARAMETERS FOR A 400 AMPERE ARC ON A
COPPER CATHODE

Cathode Temperature (Kelvin)	Plasma Temperature (eV)	Cathode Potential (Volts)	Transition Potential (Volts)	Total Arc Potential (Volts)
3500	1.47	22.22	17.91	40.13
3550	1.52	20.97	18.97	39.94
3600	1.57	19.81	20.05	39.86
3650	1.62	18.78	21.12	39.91
3700	1.67	17.87	22.20	40.07
3750	1.73	17.06	23.25	40.31
3800	1.79	16.35	24.28	40.63
3850	1.85	15.72	25.25	40.98
3900	1.92	15.18	26.16	41.34
3950	1.99	14.72	26.97	41.69
4000	2.07	14.33	27.64	41.98
4050	2.15	14.02	28.15	42.16
4100	2.24	13.77	28.42	42.20
4150	2.34	13.60	28.41	42.01
4200	2.45	13.50	28.03	41.53
Cathode Temperature (Kelvin)	Partial Pressure (atm.)	Degree of Ionization	Return Coefficient	Spot Radius (10^{-4} m)
3500	10.9	0.1535	0.4702	9.874
3550	12.6	0.1610	0.4726	8.762
3600	14.5	0.1695	0.4751	7.772
3650	16.6	0.1784	0.4777	6.903
3700	19.0	0.1877	0.4803	6.136
3750	21.6	0.1976	0.4830	5.459
3800	24.5	0.2081	0.4858	4.860
3850	27.6	0.2193	0.4888	4.327
3900	31.1	0.2314	0.4918	3.853
3950	34.9	0.2446	0.4950	3.430
4000	39.1	0.2591	0.4984	3.051
4050	43.6	0.2752	0.5021	2.710
4100	48.5	0.2934	0.5061	2.404
4150	53.8	0.3141	0.5105	2.127
4200	59.6	0.3380	0.5154	1.876

TABLE 7 (CONTINUED)
CATHODE SPOT PARAMETERS FOR A 400 AMPERE ARC ON A
COPPER CATHODE

Cathode Temperature (Kelvin)	Electric Field (10^6 V/m)	Electron Current Density (10^6 A/m 2)	Ion Current Density (10^6 A/m 2)	Total Current Density (10^6 A/m 2)
3500	2.940	0.599	0.707	1.306
3550	3.187	0.803	0.856	1.659
3600	3.456	1.072	1.036	2.108
3650	3.743	1.424	1.248	2.672
3700	4.049	1.883	1.498	3.3822
3750	4.377	2.480	1.792	4.272
3800	4.728	3.253	2.138	5.391
3850	5.107	4.256	2.544	6.800
3900	5.516	5.554	3.022	8.577
3950	5.961	7.238	3.586	10.83
4000	6.446	9.427	4.254	13.68
4050	6.980	12.28	5.047	17.33
4100	7.572	16.03	5.996	22.03
4150	8.234	21.00	7.141	28.14
4200	8.981	27.64	8.534	36.17
Cathode Temperature (Kelvin)	Ion/Total Current Density Ratio	Coulomb Logarithm	Conductivity (mho/m)	Erosion Rate (10^{27} atoms/m 2 -s)
3500	0.5415	10.5	3234	3.240
3550	0.5161	10.5	3403	3.704
3600	0.4915	10.5	3586	4.214
3650	0.4671	10.4	3779	4.775
3700	0.4431	10.4	3983	5.389
3750	0.4196	10.4	4198	6.059
3800	0.3966	10.4	4427	6.787
3850	0.3742	10.3	4671	7.575
3900	0.3524	10.3	4933	8.425
3950	0.3313	10.3	5216	9.337
4000	0.3109	10.3	5524	10.31
4050	0.2912	10.3	5861	11.35
4100	0.2722	10.3	6236	12.45
4150	0.2538	10.3	6656	13.61
4200	0.2359	10.3	7135	14.82

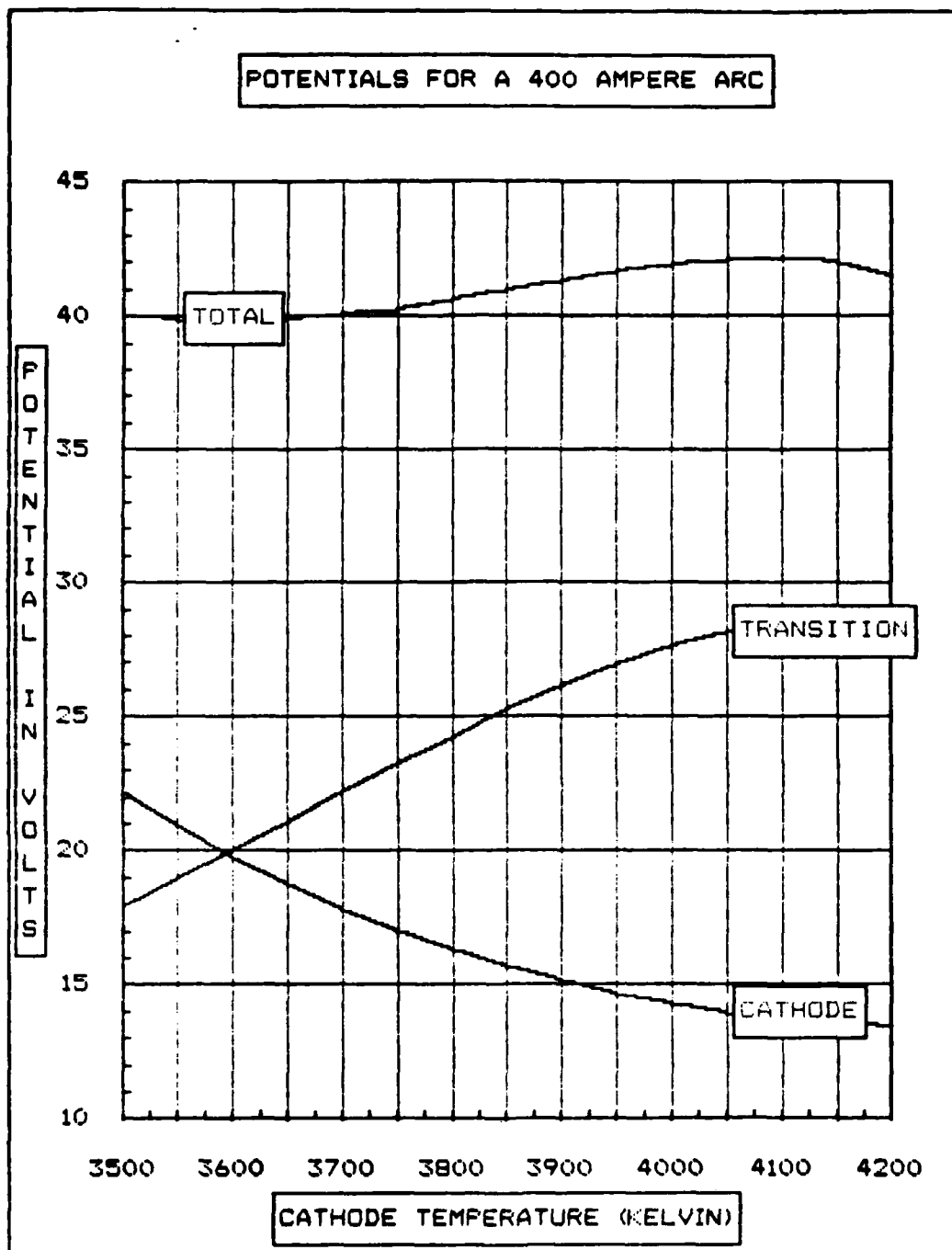


Figure 5.7 Potentials for a 400 Ampere Arc

TABLE 8
CATHODE SPOT PARAMETERS FOR STABLE ARCS

Parameter	Arc Current		
	200	300	400
Cathode Temperature (Kelvin)	3850	3700	3600
Plasma Temperature (eV)	187	168	157
Cathode Potential (Volts)	15.88	17.94	19.81
Spot Radius (10^{-4} m)	3.022	5.290	7.772
Ion Current Density (10^8 A/m ²)	2.617	1.514	1.036
Electron Current Density (10^8 A/m ²)	4.353	1.898	1.072
Total Current Density (10^8 A/m ²)	6.970	3.412	2.108
Erosion Rate (10^{27} atoms/m ² -s)	7.556	5.385	4.214

VI. CONCLUSIONS AND RECOMMENDATIONS

This study has attempted to answer some of the questions associated with the cathode phenomena in a unipolar arc. However, a more detailed analysis of the cathode spot must be accomplished before a consistent understanding of the diverse phenomena occurring within the arc can be achieved. The stationary model presented here is only a beginning and a tool for the development of future models. It can not answer the questions regarding arc initiation, extinction, and spot motion that will have to be addressed in future models if they are to be accepted. Additional research with stationary models should consider including the reverse electron current from the plasma back to the metal, changing from a constant cathode temperature in the arc radius to a constant heat flux with a varying temperature, considering the ohmic heating of the cathode spot by the electron current, and varying the cathode material parameters to determine their influence on the arc stability. It is hoped that this study will help to stimulate further interest and research into the cathode spot of a unipolar arc.

LIST OF REFERENCES

1. Chen, F. F., *Introduction to Plasma Physics and Controlled Fusion*, 2nd ed., v. 1, p. 3, Plenum Press, 1984.
2. Langmuir, I., "The Effect of Space Charge and Residual Gases on Thermionic Currents in High Vacuum," *Physical Review*, v. 2, pp. 450-486, 1913.
3. MacKeown, S. S., "The Cathode Drop in an Electric Arc," *Physical Review*, v. 34, pp. 611-614, 1929.
4. Murphy, E. L. and Good, R. H., "Thermionic Emission, Field Emission, and the Transition Region," *Physical Review*, v. 102, pp. 1464-1473, 1956.
5. Bugaev, S. P., Litvinov, E. A., Mesyats, G. A., and Proskurovskii, D. I., "Explosive Emission of Electrons," *Soviet Physics-Uspokhi*, v. 18, pp. 51-61, 1975.
6. Litvinov, E. A., Mesyats, G. A., and Proskurovskii, D. I., "Field Emission and Explosive Electron Emission Processes in Vacuum Discharges," *Soviet Physics-Uspokhi*, v. 26, pp. 138-159, 1983.
7. Fursei, G. N. and Zhukov, V. M., "Mechanism for Explosive Emission I. Emission Characteristics of Explosive Emission from Microscopic Metal Points," *Soviet Physics Technical Physics*, v. 21, pp. 176-181, 1976.
8. Zhukov, V. M. and Fursei, G. N., "Mechanism for Explosive Emission II. State of the Cathode Surface During Explosive Emission," *Soviet Physics Technical Physics*, v. 21, pp. 182-187, 1976.
9. Zhukov, V. M. and Fursei, G. N., "Explosive Electron Emission from Copper Points," *Soviet Physics Technical Physics*, v. 21, pp. 1112-1117, 1976.
10. Robson, A. E. and Thoneman, P. C., "An Arc Maintained on an Isolated Metal Plate Exposed to a Plasma," *Procedural Physics Society*, v. 73, pp. 508-512, 1959.
11. Schwirzke, F. and Taylor, R. J., "Surface Damage by Sheath Effects and Unipolar Arcs," *Journal of Nuclear Materials*, v. 93 and 94, pp. 780-784, 1980.
12. Schwirzke, F., "Unipolar Arc Model," *Journal of Nuclear Materials*, v. 128 and 129, pp. 609-612, 1984.

13. Schwirzke, F., "Unipolar Arcing, a Basic Laser Damage Mechanism," *Naval Postgraduate School Report NPS-61-83-008*, pp. 1- 21, 1983.
14. Lyubimov, G. A. and Rakhovskii, V. I., "The Cathode Spot of a Vacuum Arc," *Soviet Physics-Uspexhi*, v. 21, pp. 693-718, 1978.
15. Hantzshe, E., "Theory of Cathode Spot Phenomena," *Physica*, v. 104C, pp. 3-16, 1981.
16. Lee, T. H. and Greenwood, A., "Theory for the Cathode Mechanism in Metal Vapor Arcs," *Journal of Applied Physics*, v. 32, pp. 916-923, 1961.
17. Kulyapin, V. M., "Quantitative Theory of Cathode Processes in an Arc," *Soviet Physics Technical Physics*, v. 16, pp. 287-291, 1971.
18. Kubono, T., "A Theory for the Cathode Mechanism in Low-Current Vacuum Arcs, with Application to the Calculation of Erosion Rate," *Journal of Applied Physics*, v. 49, pp. 3863-3869, 1978.
19. Beilis, I., "Analysis of the Cathode Spot in a Vacuum Arc," *Soviet Physics Technical Physics*, v. 19, pp. 251-256, 1974.
20. Moizhes, B. Ya. and Nemchinskii, V. A., "Theory of a High-Pressure Arc with a Refractory Cathode," *Soviet Physics Technical Physics*, v. 17, pp. 793-799, 1972.
21. Moizhes, B. Ya. and Nemchinskii, V. A., "High-Pressure Arc with a Refractory Cathode. II," *Soviet Physics Technical Physics*, v. 18, pp. 1460-1464, 1974.
22. Nemchinskii, V. A., "Theory of the Vacuum Arc," *Soviet Physics Technical Physics*, v. 24, pp. 764-767, 1979.
23. Nemchinskii, V. A., "Comparison of Calculated and Experimental Results for a Stationary Cathode Spot in a Vacuum Arc," *Soviet Physics Technical Physics*, v. 28, pp. 1449-1451, 1979.
24. Nemchinskii, V. A., "Monte Carlo Calculation of the Erosion Rate and Ion Current at a Vacuum Arc Cathode," *Soviet Physics Technical Physics*, v. 27, pp. 1073-1077, 1982.
25. Ecker, G., "Theoretical Aspects of the Vacuum Arc," *Vacuum Arcs Theory and Application* Laferty, J. M., Editor; John Wiley & Sons, pp. 228-320, 1980.
26. Hoyaux, M. F., *Arc Physics*, Springer-Verlag New York Inc., pp. 299-301, 1968.

27. Honig, R. E., "Vapor Pressure Data for the More Common Elements," *RCA Review*, pp. 195-204, 1957.

APPENDIX A GENERAL EMISSION PROGRAM

```
C ****
C *
C *      EMM1.EXE
C *
C *      PURPOSE
C *      CALCULATE THE ELECTRON CURRENT DENSITY
C *      EMITTED FOR A RANGE OF ELECTRIC FIELDS AT
C *      THE SURFACE OF A CATHODE WITH A GIVEN WORK
C *      FUNCTION AND CATHODE TEMPERATURE.
C *
C *      DESCRIPTION OF VARIABLES
C *      T      CATHODE TEMPERATURE
C *      F      ELECTRIC FIELD
C *      F0     INITIAL ELECTRIC FIELD
C *      PHI    WORK FUNCTION
C *      DF     ELECTRIC FIELD INCREMENT
C *      J      CURRENT DENSITY
C *      ECODE   ERROR CODE
C *              0 = GOOD
C *              1 = ERROR
C *      TYP    TYPE OF EMISSION
C *              1= THERMIONIC
C *              2= INTERMEDIATE
C *              3= FIELD
C *              4= NONE
C *
C *      SUBROUTINES REQUIRED
C *      EMMAPP(T,F,PHI,TYP)
C *      TFEMM1(T,F,PHI,J,ECODE)
C *      IFTEMM1(T,F,PHI,J,ECODE)
C *      FTEMM1(T,F,PHI,J,ECODE)
C *
C ****
```

```
REAL*8 T,F,F0,PHI,DF,J
INTEGER I,N,ECODE,TYP
OPEN(4,FILE='CON')
OPEN(6,FILE='EMM1.DAT',STATUS='NEW')
WRITE(*,*) 'ENTER THE NUMBER OF DATA POINTS:'
READ(*,*) N
WRITE(*,*) 'ENTER THE ABSOLUTE TEMPERATURE (K):'
READ(*,*) T
WRITE(*,*) 'ENTER INITIAL ELECTRIC FIELD (V/M):'
READ(*,*) F0
WRITE(*,*) 'ENTER ELECTRIC FIELD INCREMENT (V/M):'
READ(*,*) DF
```

```
      WRITE(*,*) 'ENTER WORK FUNCTION (eV): '
      READ(*,*) PHI
      F=F0
      J=0.
      DO 20 I=1,N
         CALL EMMAPP(T,F,PHI,TYP)
         IF(TYP.EQ.1) CALL TFEMM1(T,F,PHI,J,ECODE)
         IF(TYP.EQ.2) CALL IFTEMM1(T,F,PHI,J,ECODE)
         IF(TYP.EQ.3) CALL FTEMM1(T,F,PHI,J,ECODE)
         IF(TYP.EQ.4) GOTO 10
         WRITE(6,900) F, J, ECODE, TYP
10      F=F + DF
20      CONTINUE
      STOP
900     FORMAT(1X,D12.6,5X,D12.6,5X,I5,5X,I5)
      END
```

APPENDIX B GENERAL EMISSION SUBROUTINE

```
C ****
C *
C *      SUBROUTINE EMM
C *
C *      PURPOSE
C *      CALCULATE THE ELECTRON CURRENT DENSITY
C *      FOR A GIVEN ELECTRIC FIELD AT THE SURFACE
C *      OF A CATHODE WITH A GIVEN WORK FUNCTION AND
C *      CATHODE TEMPERATURE.
C *
C *      DESCRIPTION OF VARIABLES
C *      T      CATHODE TEMPERATURE
C *      F      ELECTRIC FIELD
C *      PHI    WORK FUNCTION
C *      J      CURRENT DENSITY
C *      ECODE   ERROR CODE
C *              0 = GOOD
C *              1 = ERROR
C *      TYP    TYPE OF EMISSION
C *              1= THERMIONIC
C *              2= INTERMEDIATE
C *              3= FIELD
C *              4= NONE
C *
C *      SUBROUTINES REQUIRED
C *      EMMAPP(T,F,PHI,TYP)
C *      TFEMM1(T,F,PHI,J,ECODE)
C *      IFTEMM1(T,F,PHI,J,ECODE)
C *      FTEMM1(T,F,PHI,J,ECODE)
C *
C ****
```

```
SUBROUTINE EMM(T,F,PHI,J,ECODE,TYP)
REAL*8 T,F,PHI,J
INTEGER ECODE,TYP
CALL EMMAPP(T,F,PHI,TYP)
IF(TYP.EQ.1) CALL TFEMM1(T,F,PHI,J,ECODE)
IF(TYP.EQ.2) CALL IFTEMM1(T,F,PHI,J,ECODE)
IF(TYP.EQ.3) CALL FTEMM1(T,F,PHI,J,ECODE)
RETURN
END
```

APPENDIX C EMISSION APPLICABILITY SUBROUTINE

```

*****
*          SUBROUTINE EMMAPP
*
*          PURPOSE
*              DETERMINES APPLICABILITY OF THE SUBROUTINES
*              TFEMM1, IFTEMM1, AND FTEMM1
*
*          DESCRIPTION OF VARIABLES
*              T      CATHODE TEMPERATURE
*              F0     ELECTRIC FIELD AT CATHODE SURFACE
*              PHI0   WORK FUNCTION
*              TYP    TYPE OF EMISSION
*                     1= THERMIONIC
*                     2= INTERMEDIATE
*                     3= FIELD
*                     4= NONE
*
*          SUBROUTINES REQUIRED
*              NONE
*
*****
```

SUBROUTINE EMMAPP(T,F0,PHI0,TYP)
REAL*8 T,F,PHI,M,E,K,H,EPS,PI,PHI0,D,D1
REAL*8 F0,E1,F1,KT0,KT,Y,YE,TY,TE,V,VE,ETA,ETA0
REAL*8 TEST1,TEST2,TEST3,TEST4
INTEGER ECODE1,ECODE2,ECODE3,TYP,N
M=9.1095E-31
E=1.6022E-19
K=1.3807E-23
H=1.0546E-34
EPS=8.8542E-12
PI=3.141592654
E1=(4*PI*EPS*H)**2/(M*E**4)
F1=E1**2*E**3/(4*PI*EPS)
F=F0*F1
KT0=K*T
KT=KT0*E1
PHI=PHI0*E1*E
N=0
D=F**(.4.)/(PI*KT)
IF(1-D) 20,20,10
10 TEST1=DLOG((1-D)/D)-1/(D*(1-D))
TEST2=-PI/(F**(.4.))*(PHI-DSQRT(F))
TEST3=DLOG((1-D)/D)-1/(1-D)

```

TEST4=-PI/(F**(1./8.))
IF((TEST1.GT.TEST2).AND.(TEST3.GT.TEST4)) THEN
    ECODE1=0
ELSE
    ECODE1=1
ENDIF
GOTO 30
20 ECODE1=1
30 ETA0=-F**2/(8*KT**2)
Y=DSQRT(F)/PHI
CALL VTY(Y,V,TY,IER1)
40 YE=DSQRT(F)/(-ETA0)
CALL VTY(YE,VE,TE,IER2)
ETA=-F**2/(8*KT**2*TE**2)
IF(DABS(ETA-ETA0).GT. 1.0D-6) THEN
    ETA0=ETA-(ETA-ETA0)/2.1
    N=N+1
    IF(N.GT.200) THEN
        ECODE2=1
        GOTO 50
    ENDIF
    GOTO 40
ENDIF
D=2*DSQRT(2/YE)*TE/PI
TEST1=1/YE
TEST2=1 + F**(1./4.)*D/(PI*(D-1))
TEST3=-F**2/(8*KT**2*TE**2)
TEST4=-PHI+KT/(1-F/(2*DSQRT(2*PHI)*KT*TY))
IF((TEST1.GT.TEST2).AND.(TEST3.GT.TEST4)) THEN
    ECODE2=0
ELSE
    ECODE2=1
ENDIF
50 D=(2*DSQRT(2.0*PHI)*PI*KT)/F
D1=4*DSQRT(2*PHI)*PHI/(3*F)
TEST1=PHI-DSQRT(F)
TEST2=F**(3./4.)/PI + KT/(1-D*TY/PI)
TEST3=1-D*TY/PI
TEST4=KT*DSQRT((V*PHI/F)*DSQRT(2*PHI)/(PHI**2-F))
IF((TEST1.GT.TEST2).AND.(TEST3.GT.TEST4)) THEN
    ECODE3=0
ELSE
    ECODE3=1
ENDIF
IF(ECODE1.EQ.0) THEN
    TYP=1
ELSE
    IF(ECODE2.EQ.0) THEN
        TYP=2
    ELSE
        IF(ECODE3.EQ.0) THEN

```

```
TYP=3
ELSE
    TYP=4
ENDIF
ENDIF
RETURN
END
```

APPENDIX D T-E EMISSION SUBROUTINE

```
C ****
C *
C *      SUBROUTINE TFEMM1
C *
C *      PURPOSE
C *          CALCULATES THE ELECTRON CURRENT DENSITY
C *          FOR THERMIONIC FIELD EMISSION
C *
C *      DESCRIPTION OF VARIABLES
C *          T      CATHODE TEMPERATURE
C *          F0     ELECTRIC FIELD AT CATHODE SURFACE
C *          PHI0   WORK FUNCTION
C *          J0     CURRENT DENSITY
C *          ECODE  ERROR CODE
C *                  0= GOOD
C *                  1= ERROR
C *
C *      SUBROUTINES REQUIRED
C *          NONE
C *
C ****
C
C SUBROUTINE TFEMM1(T,F0,PHI0,J0,ECODE)
REAL*8 T,F,PHI,J,M,E,K,H,PI,PHI0,D
REAL*8 F0,J0,E1,F1,J1,KT0,KT
REAL*8 TEST1,TEST2,TEST3,TEST4
INTEGER ECODE
M=9.1095E-31
E=1.6022E-19
K=1.3807E-23
H=1.0546E-34
EPS=8.8542E-12
PI=3.141592654
E1=(4*PI*EPS*H)**2/(M*E**4)
F1=E1**2*E**3/(4*PI*EPS)
J1=E1**2*H**3/(M*E)
F=F0*F1
KT0=K*T
KT=KT0*E1
PHI=PHI0*E1*E
D=F***(3./4.)/(PI*KT)
J=(KT**2/(2*PI**2))*((PI*D)/DSIN(PI*D))*1
1    DEXP(-(PHI-DSQRT(F))/KT)
J0=J/J1
IF(1-D) 20,20,10
20  TEST1=DLOG((1-D)/D)-1/(D*(1-D))
10
```

```
TEST2=-PI/(F**(3./4.))*(PHI-DSQRT(F))
TEST3=DLOG((1-D)/D)-1/(1-D)
TEST4=-PI/(F**(1./8.))
IF((TEST1.GT.TEST2).AND.(TEST3.GT.TEST4)) THEN
    ECODE=0
ELSE
    ECODE=1
ENDIF
RETURN
20 ECODE=1
RETURN
END
```

APPENDIX E FIELD-THERMIONIC EMISSION SUBROUTINE

```
C ****
C *
C *      SUBROUTINE FTEMM1
C *
C *      PURPOSE
C *          CALCULATES THE ELECTRON CURRENT DENSITY
C *          FOR FIELD-THERMIONIC EMISSION
C *
C *      DESCRIPTION OF VARIABLES
C *          T      CATHODE TEMPERATURE
C *          F0     ELECTRIC FIELD AT CATHODE SURFACE
C *          PHI0   WORK FUNCTION
C *          J0     CURRENT DENSITY
C *          ECODE  ERROR CODE
C *                  0= GOOD
C *                  1= ERROR
C *
C *      SUBROUTINES REQUIRED
C *          VTY(Y,V,TY,IER)
C *
C ****
C
C SUBROUTINE FTEMM1(T,F0,PHI0,J0,ECODE)
REAL*8 T,F,PHI,J,M,E,K,H,EPS,PI,PHI0,D,D1,TY
REAL*8 TEST1,TEST2,TEST3,TEST4,Y,V,C1,C2,C3
REAL*8 F0,J0,E1,F1,J1,KTO,KT
INTEGER ECODE
M=9.1095E-31
E=1.6022E-19
K=1.3807E-23
H=1.0546E-34
EPS=8.8542E-12
PI=3.141592654
E1=(4*PI*EPS*H)**2/(M*E**4)
F1=E1**2*E**3/(4*PI*EPS)
J1=E1**2*H**3/(M*E)
F=F0*F1
KTO=K*T
KT=KT0*E1
PHI=PHI0*E1*E
D=(2*DSQRT(2.0*PHI)*PI*KT)/F
D1=4*DSQRT(2*PHI)*PHI/(3*F)
Y=DSQRT(F)/PHI
CALL VTY(Y,V,TY,IER)
J=F**2*(D*TY/DSIN(D*TY))*DEXP(-D1*V)/(16*PI**2*PHI*TY**2)
J0=J/J1
```

```
TEST1=PHI-DSQRT(F)
TEST2=F**(3./4.)/PI + KT/(1-D*TY/PI)
TEST3=1-D*TY/PI
TEST4=KT*DSQRT((V*PHI/F)*DSQRT(2*PHI)/(PHI**2-F))
IF((TEST1.GT.TEST2).AND.(TEST3.GT.TEST4)) THEN
    ECODE=0
ELSE
    ECODE=1
ENDIF
RETURN
END
```

APPENDIX F COMPLETE ELLIPTIC INTEGRAL OF THE 1ST KIND

C *****
C SUBROUTINE CEL1
C
C PURPOSE
C CALCULATE COMPLETE ELLIPTIC INTEGRAL OF FIRST
C KIND
C
C USAGE
C CALL CEL1(RES,AK,IER)
C
C DESCRIPTION OF PARAMETERS
C RES - RESULT VALUE
C AK - MODULUS (INPUT)
C IER - RESULTANT ERROR CODE WHERE
C IER=0 NO ERROR
C IER=1 AK NOT IN RANGE -1 TO +1
C
C REMARKS
C THE RESULT IS SET TO 1E75 IF ABS(AK) GE 1
C FOR MODULUS AK AND COMPLEMENTARY MODULUS CK,
C EQUATION AK*AK+CK*CK=1.0 IS USED.
C AK MUST BE IN THE RANGE -1 TO +1
C
C SUBROUTINES AND FUNCTION SUBPROGRAMS REQUIRED
C NONE
C
C METHOD
C DEFINITION
C CEL1(AK)=INTEGRAL(1/SQRT((1+T*T)*(1+(CK*T)**2)),
C SUMMED OVER T FROM 0 TO INFINITY).
C EQUIVALENT ARE THE DEFINITIONS
C CEL1(AK)=INTEGRAL(1/(COS(T)SQRT(1+(CK*TAN(T))**2)))
C SUMMED OVER T FROM 0 TO PI/2),
C CEL1(AK)=INTEGRAL(1/SQRT(1-(AK*SIN(T))**2)),
C SUMMED OVER T FROM 0 TO PI/2), WHERE
C K=SQRT(1-CK*CK).
C EVALUATION
C LANDENS TRANSFORMATION IS USED FOR CALCULATION.
C REFERENCE
C R.BULIRSCH, 'NUMERICAL CALCULATION OF ELLIPTIC
C INTEGRALS AND ELLIPTIC FUNCTIONS', HANDBOOK SERIES
C SPECIAL FUNCTIONS, NUMERISCHE MATHEMATIK VOL. 7,
C 1965, PP. 78-90.

C
C
C

```
*****  
SUBROUTINE CEL1(RES,AK,IER)  
REAL*8 ARI,GEO,AK,RES,AARI  
IER=0  
ARI=2.  
GEO=(0.5-AK)+0.5  
GEO=GEO+GEO*AK  
RES=0.5  
IF(GEO)1,2,4  
1 IER=1  
2 RES=1E38  
RETURN  
3 GEO=GEO*AARI  
4 GEO=DSQRT(GEO)  
GEO=GEO+GEO  
AARI=ARI  
ARI=ARI+GEO  
RES=RES+RES  
IF(GEO/AARI-0.9999)3,5,5  
5 RES=RES/ARI*6.283185E0  
RETURN  
END
```

APPENDIX G COMPLETE ELLIPTIC INTEGRAL OF 2ND KIND

C SUBROUTINE CEL2

C PURPOSE

C COMPUTES THE GENERALIZED COMPLETE ELLIPTIC
C INTEGRAL OF SECOND KIND.

C USAGE

C CALL CEL2(RES,AK,A,B,IER)

C DESCRIPTION OF PARAMETERS

C	RES	- RESULT VALUE
C	AK	- MODULUS (INPUT)
C	A	- CONSTANT TERM IN NUMERATOR
C	B	- FACTOR OF QUADRATIC TERM IN NUMERATOR
C	IER	- RESULTANT ERROR CODE WHERE
C		IER=0 NO ERROR
C		IER=1 AK NOT IN RANGE -1 TO +1

C REMARKS

C FOR ABS(AK) GE 1 THE RESULT IS SET TO 1E75 IF B
C IS POSITIVE, TO -1E75 IF B IS NEGATIVE.

C SPECIAL CASES ARE

C K(K) OBTAINED WITH A = 1, B = 1

C E(K) OBTAINED WITH A = 1, B = CK*CK WHERE CK IS
C COMPLEMENTARY MODULUS.

C B(K) OBTAINED WITH A = 1, B = 0

C D(K) OBTAINED WITH A = 0, B = 1

WHERE K, E, B, D DEFINE SPECIAL CASES OF THE
GENERALIZED COMPLETE ELLIPTIC INTEGRAL OF SECOND
KIND IN THE USUAL NOTATION, AND THE ARGUMENT K OF
THESE FUNCTIONS MEANS THE MODULUS.

C SUBROUTINES AND FUNCTION SUBPROGRAMS REQUIRED
C NONE

C METHOD

C DEFINITION

C RES=INTEGRAL((A+B*T*T)/(SQRT((1+T*T)*
C *(1+(CK*T)**2))*(1+T*T)))

C SUMMED OVER T FROM 0 TO INFINITY).

EVALUATION

LANDENS TRANSFORMATION IS USED FOR CALCULATION.

CHAPTER 1
REFERENCE

C
C
C
C
C R.BULIRSCH, 'NUMERICAL CALCULATION OF ELLIPTIC
C INTEGRALS AND ELLIPTIC FUNCTIONS', HANDBOOK SERIES
C SPECIAL FUNCTIONS, NUMERISCHE MATHEMATIK VOL. 7,
C 1965, PP. 78-90.

C
C *****
C

```
SUBROUTINE CEL2(RES,AK,A,B,IER)
REAL*8 RES,AK,A,B,ARI,GEO,A1,B0,AARI
IER=0
ARI=2.
GEO=(0.5-AK)+0.5
GEO=GEO+GEO*AK
RES=A
A1=A+B
B0=B+B
IF(GEO)1,2,6
1 IER=1
2 IF(B)3,8,4
3 RES=-1E38
RETURN
4 RES=1E38
RETURN
5 GEO=GEO*AARI
6 GEO=DSQRT(GEO)
GEO=GEO+GEO
AARI=ARI
ARI=ARI+GEO
B0=B0+RES*GEO
RES=A1
B0=B0+B0
A1=B0/ARI+A1
IF(GEO/AARI-0.9999)5,7,7
7 RES=A1/ARI
RES=RES+0.5707963E0*RES
8 RETURN
END
```

APPENDIX H FOWLER-NORDHIEM ELLIPTIC FUNCTIONS

```
C ****
C *
C *      SUBROUTINE VTY
C *
C *      PURPOSE
C *          CALCULATES THE FOWLER-NORDHIEM ELLIPTIC
C *          FUNCTIONS
C *
C *      DESCRIPTION OF VARIABLES
C *          Y      FUNCTION ARGUMENT
C *          V      FOWLER-NORDHIEM ELLIPTIC V
C *          TY     FOWLER-NORDHIEM ELLIPTIC T
C *          IER    ERROR CODE
C *          0= GOOD
C *          1= ERROR
C *
C *      SUBROUTINES REQUIRED
C *          CEL1(RES,AK,IER)
C *          CEL2(RES,AK,A,B,IER)
C *
C ****
C
C SUBROUTINE VTY(Y,V,TY,IER)
REAL*8 Y,V,TY,C1,C2,C3
INTEGER IER,IER1,IER2
IF(Y.GT. 1.0) THEN
    C1=DSQRT((Y-1)/(2*Y))
    CALL CEL1(C2,C1,IER1)
    CALL CEL2(C3,C1,1.0D00,1.0D00-C1*C1,IER2)
    V=-DSQRT(Y/2)*(-2*C3 + (Y+1)*C2)
    TY=1/DSQRT(1+Y)*((1+Y)*C3 - Y*C2)
ELSE
    C1=DSQRT((1-Y)/(1+Y))
    CALL CEL1(C2,C1,IER1)
    CALL CEL2(C3,C1,1.0D00,1.0D00-C1*C1,IER2)
    V=DSQRT(1+Y)*(C3-Y*C2)
    TY=1/DSQRT(1+Y)*((1+Y)*C3 - Y*C2)
ENDIF
IF((IER1.EQ.1).OR.(IER2.EQ.1)) THEN
    IER=1
ELSE
    IER=0
ENDIF
RETURN
END
```

APPENDIX I INTERMEDIATE F-T EMISSION SUBROUTINE

```
C ****
C *
C *        SUBROUTINE IFTEMM1
C *
C *        PURPOSE
C *        CALCULATES THE ELECTRON CURRENT DENSITY
C *        FOR INTERMEDIATE FIELD-THERMIONIC EMISSION
C *
C *        DESCRIPTION OF VARIABLES
C *        T            CATHODE TEMPERATURE
C *        F0          ELECTRIC FIELD AT CATHODE SURFACE
C *        PHI0        WORK FUNCTION
C *        J0          CURRENT DENSITY
C *        ECODE        ERROR CODE
C *                    0= GOOD
C *                    1= ERROR
C *
C *        SUBROUTINES REQUIRED
C *        VTY(Y,V,TY,IER)
C *
C ****
C
C SUBROUTINE IFTEMM1(T,F0,PHI0,J0,ECODE)
REAL*8 T,F,PHI,J,M,E,K,H,EPS,PI,PHI0,D,TE,TY
REAL*8 TEST1,TEST2,TEST3,TEST4,Y,V,C1,C2,C3,VE
REAL*8 F0,J0,E1,F1,J1,KT0,KT,ETA,ETA0,YE,THETA
INTEGER ECODE
M=9.1095E-31
E=1.6022E-19
K=1.3807E-23
H=1.0546E-34
EPS=8.8542E-12
PI=3.141592654
E1=(4*PI*EPS*H)**2/(M*E**4)
F1=E1**2*E**3/(4*PI*EPS)
J1=E1**2*H**3/(M*E)
F=F0*F1
KT0=K*T
KT=KT0*E1
PHI=PHI0*E1*E
ETA0=-F**2/(8*KT**2)
Y=DSQRT(F)/PHI
CALL VTY(Y,V,TY,IER1)
20 YE=DSQRT(F)/(-ETA0)
CALL VTY(YE,VE,TE,IER2)
ETA=-F**2/(8*KT**2*TE**2)
```

```
IF(DABS(ETA-ETA0).GT. 1.0D-6) THEN
    ETA0=ETA-(ETA-ETA0)/2.1
    GOTO 20
ENDIF
THETA=3/(TE**2) - 2*VE/(TE**3)
J=F*DSQRT(KT*TE/(2*PI))/(2*PI)*DEXP(-PHI/KT + F**2*
1  THETA/(24*KT**3))
J0=J/J1
D=2*DSQRT(2/YE)*TE/PI
TEST1=1/YE
TEST2=1 + F**2*(1/4.)*D/(PI*(D-1))
TEST3=-F**2/(8*KT**2*TE**2)
TEST4=-PHI+KT/(1-F/(2*DSQRT(2*PHI)*KT*TY))
IF((TEST1.GT.TEST2).AND.(TEST3.GT.TEST4)) THEN
    ECODE=0
ELSE
    ECODE=1
ENDIF
RETURN
END
```

APPENDIX J ARC PROGRAM

```
C ****
C *
C *      ARC.EXE
C *
C *      PURPOSE
C *      DETERMINES THE CHARACTERISTIC VALUES FOR
C *      THE CATHODE SPOT OF AN ARC BURNING ON A
C *      COPPER PLATE
C *
C *      DESCRIPTION OF VARIABLES
C *      LO      HEAT OF VAPORIZATION
C *      PO      PARTIAL PRESSURE CONSTANT
C *      MI      MASS OF COPPER ATOM
C *      EI      IONIZATION POTENTIAL ENERGY
C *      PHIO    WORK FUNCTION (EV)
C *      BETA   FRACTION ENERGY REMOVED WITH
C *              COULOMB INTERACTION
C *      XI     THERMAL CONDUCTIVITY
C *      EER    EROSION ENERGY
C *      Z      AVERAGE ION CHARGE
C *      NO     AVOGADRO'S NUMBER
C *      M      ELECTRON MASS
C *      E      ELECTRON CHARGE
C *      K      BOLTZMAN'S CONSTANT
C *      H      PLANCK'S CONSTANT
C *      EPS    PERMITIVITY OF FREE SPACE
C *      ATP    DEGREE OF IONIZATION
C *      ETA    VAPORIZATION RETURN COEFFICIENT
C *      F      ELECTRIC FIELD AT CATHODE SURFACE
C *      G      EROSION RATE
C *      PHI   SCHOTTKY CORRECTED WORK FUNCTION
C *      PI     PI
C *      PTK    VAPOR PARTIAL PRESSURE
C *      R      RADIUS OF CATHODE SPOT
C *      SIG   PLASMA CONDUCTIVITY
C *      TK    CATHODE TEMPERATURE (K)
C *      U     POTENTIAL DROP IN QUASINEUTRAL
C *              PLASMA
C *      VK    CATHODE POTENTIAL DROP
C *      VT    TOTAL POTENTIAL DROP ACROSS ARC
C *      J     TOTAL CURRENT DENSITY
C *      JE   ELECTRON CURRENT DENSITY
C *      JI   ION CURRENT DENSITY
C *      KTK  CATHODE TEMPERATURE (JOULES)
C *      KTP  PLASMA TEMPERATURE (JOULES)
C *      I    ARC CURRENT
```

```

C * ND NUMBER OF DATA SETS
C * DTK CATHODE TEMPERATURE INCREMENT
C * COULOG COULOMB LOGARITHM
C * ECODE ERROR CODE
C * 0= GOOD
C * 1= ERROR
C * TYP TYPE OF EMISSION
C * 1= THERMIONIC
C * 2= INTERMEDIATE
C * 3= FIELD
C * 4= NONE
C *
C * SUBROUTINES REQUIRED
C * EMM(T,F,PHIO,J,ECODE,TYPE)
C *
*****  

C  

REAL*8 L0,P0,MI,EI,PHIO,BETA,XI,EER,Z,N0,M,E,K,H,EP  

REAL*8 ATP,ETA,F,G,PHI,PI,PTK,R,SIG,TK,U,VK,VK1,VK2,VT  

REAL*8 S1,S2,S3,S4,S5,J,JE,JI,KTK,KTP,I,DTK,COULOG  

INTEGER ECODE,TYP,N,ND  

OPEN(6,FILE='ARC.DAT',STATUS='NEW')  

OPEN(7,FILE='PRN')  

WRITE(*,*) 'ENTER NUMBER OF DATA SETS:  

READ(*,*) ND  

WRITE(*,*) 'ENTER INITIAL PLASMA TEMPERATURE (EV):'  

READ(*,*) KTP  

WRITE(*,*) 'ENTER INITIAL CATHODE TEMPERATURE (K):'  

READ(*,*) TK  

WRITE(*,*) 'ENTER CATHODE TEMPERATURE INCREMENT (K):'  

READ(*,*) DTK  

WRITE(*,*) 'ENTER ARC CURRENT (A):'  

READ(*,*) I  

WRITE(6,900) ND,I  

WRITE(7,900) ND,I  

MI=63.54  

L0=300300.  

EI=12377D-18  

PHIO=4.4  

XI=40.  

BETA=3.21  

Z=18  

N0=6.0220D23  

M=9.1095D-31  

E=16022D-19  

K=13807D-23  

H=6.6262D-34  

PI=3.141592654  

EPS=8.8542D-12  

EER=L0/N0  

S1=-1.7520D4

```

RD-R190 189

THEORETICAL MODEL OF THE CATHODE SPOT ON A UNIPOLAR ARC
(U) NAVAL POSTGRADUATE SCHOOL MONTEREY CA D H CURTISS

2/2

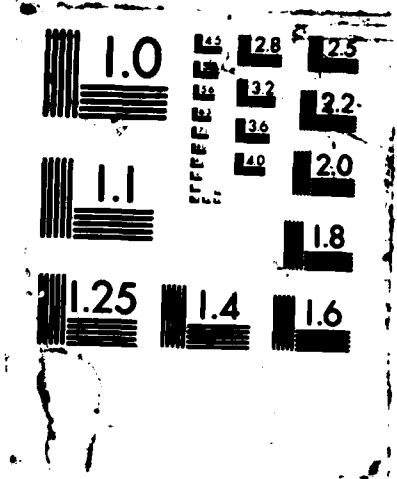
DEC 87

UNCLASSIFIED

F/G 20/3

ML





```

S2=-1.21
S3=0
S4=13.21
S5=133.322368421
VK=15.
MI=MI*1.6726D-27
KTP=E*KTP
DO 20 N=1,ND
KTK=K*TK
JE=0.
PTK=(10**((S1/TK + S2*DLOG10(TK)+S3*TK+S4))*S5
10 ATP=1/DSQRT(1 + PTK/KTP*(2*PI*H**2/(M*KTP))**(.2.)*
1      DEXP(EI/KTP))
1      ETA=(8./3. + ATP-DSQRT(5.*PI*KTK/(6.*KTP)))/
1      (8./3. + ATP+DSQRT(5.*PI/6.))
JI=E*PTK*ETA*ATP/DSQRT(2*PI*MI*KTK)
F=DSQRT(JI*DSQRT(8*VK*MI/E)/EPS*(1-JE/JI*DSQRT(M/MI)))
PHI=PHIO*E-DSQRT(E**3*F/(4*PI*EPS))
CALL EMM(TK,F,PHIO,JE,ECODE,TYP)
R=DSQRT(I/(PI*(JE+JI)))
VK1=((JI/JE)*(EI+2*KTP)+BETA*KTP*(1+JI/JE)-2*KTK)/E
G=PTK*(1-ETA)/DSQRT(2*PI*MI*KTK)
VK2=4*XI*TK/(PI*R*JI)+((JE/JI)*(PHI+2*KTK)+(G/JI)*EER*E
1      -EI-2*KTP+PHI)/E
IF(DABS(VK2-VK1).GT. 10D-1) THEN
    IF(VK2.GT.VK1) THEN
        VK=VK1
        IF(DABS(VK2-VK1).GT. 100) THEN
            KTP=KTP+100.*K
        ELSE
            KTP=KTP+DABS(VK2-VK1)*K
        ENDIF
    ELSE
        VK=VK2
        IF(DABS(VK2-VK1).GT. 100) THEN
            KTP=KTP-101.*K
        ELSE
            KTP=KTP-DABS(VK2-VK1)*K
        ENDIF
    ENDIF
    IF(VK.LT.0) VK=DABS(VK)
    GOTO 10
ENDIF
VK=(VK1+VK2)/2
J=JE+JI
COULOG=23.0-DLOG(DSQRT(PTK*ATP*ETA/K)/(KTP/K)**2)
SIG=153D-2*(KTP/K)**(.2.)/COULOG
U=(I*E*G/(2*PI*SIG*R*J))*(1+Z)/(1+(E*G/J)*(1+Z))-1
1      BETA*(KTP/E)/(1.+(E*G/J)*(1.+Z))
VT=VK+U
WRITE(6,910) TK,KTP/E,VK,U,VT

```

```
      WRITE(6,920) PTK/1.01D5,ATP,ETA,JI/J,R
      WRITE(6,930) F,JE,JI,J
      WRITE(6,940) COULOG, SIG, G
      WRITE(7,910) TK,KTP/E,VK,U,VT
      WRITE(7,920) PTK/1.01D5,ATP,ETA,JI/J,R
      WRITE(7,930) F,JE,JI,J
      WRITE(7,940) COULOG,SIG,G
      TK=TK+DTK
 20  CONTINUE
      STOP
 900  FORMAT(1X,I3.5X,F4.0)
 910  FORMAT(1X,F5.0,5X,F6.2,5X,F6.2,5X,F6.2,5X,F6.2)
 920  FORMAT(1X,F4.1,5X,F6.4,5X,F6.4,5X,F6.4,5X,1P,D10.4)
 930  FORMAT(1X,1P,D10.4,5X,D10.4,5X,D10.4,5X,D10.4)
 940  FORMAT(1X,F4.1,5X,F7.1,5X,1P,D10.4)
      END
```

INITIAL DISTRIBUTION LIST

	No. Copies
1. Defense Technical Information Center Cameron Station Alexandria, Virginia 22304-6145	2
2. Library, Code 0142 Naval Postgraduate School Monterey, California 93943-5002	2
3. Professor F. R. Schwirzke, Code 61Sw Department of Physics Naval Postgraduate School Monterey, California 93943-5002	2
4. Professor K. E. Woehler, Code 61Wh Department of Physics Naval Postgraduate School Monterey, California 93943-5002	1
5. Lieutenant Dwayne H. Curtiss Naval Submarine School Code 20 SOAC 88030 Box 700 Groton, Connecticut 06349	2

END
DATE
FI / MED

4-88

DTIC